iScience

Article

Supinoxin blocks small cell lung cancer progression by inhibiting mitochondrial respiration through DDX5

Graphical abstract

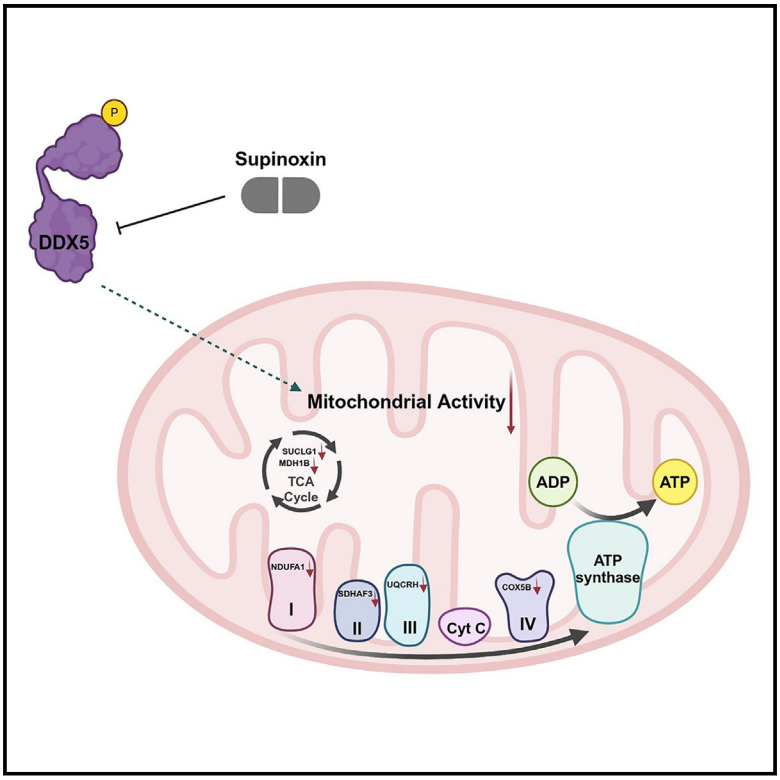

Highlights

- The overexpression of DDX5 in SCLC is due to increased protein stability
- Supinoxin inhibits the proliferation of SCLC both *in vivo* and *in vitro*
- Supinoxin and DDX5 knockdown impair expression of mitochondrial respiration genes
- Supinoxin induces mitochondrial dysfunction in chemo resistant SCLC cells

Authors

Subhadeep Das, Maria P. Zea, Matthew P. Russon, ..., Haley Anne Harper, Bennett D. Elzey, Elizabeth J. Tran

Correspondence

ejtran@purdue.edu (B.D.E.), belzey@purdue.edu (E.J.T.)

In brief

Molecular biology; Cancer; Transcriptomics

Das et al., 2025, iScience *28*, 112219
April 18, 2025
https://doi.org/10.1016/j.isci.2025.112219

CellPress

iScience

CellPress
OPEN ACCESS

Article

Supinoxin blocks small cell lung cancer progression by inhibiting mitochondrial respiration through DDX5

Subhadeep Das,[1,2] Maria P. Zea,[1] Matthew P. Russon,[1] Zheng Xing,[1] Sandra Torregrosa-Allen,[2] Heidi E. Cervantes,[2] Haley Anne Harper,[2] Bennett D. Elzey,[2,3,*] and Elizabeth J. Tran[1,2,4,*]

[1]Department of Biochemistry, Purdue University, BCHM A343, 175 S. University Street, West Lafayette, IN 47907-2063, USA
[2]Purdue University Institute for Cancer Research, Purdue University, Hansen Life Sciences Research Building, Room 141, 201 S. University Street, West Lafayette, IN 47907-2064, USA
[3]Department of Comparative Pathobiology, Purdue University, West Lafayette, IN, USA
[4]Lead contact
*Correspondence: ejtran@purdue.edu (B.D.E.), belzey@purdue.edu (E.J.T.)
https://doi.org/10.1016/j.isci.2025.112219

SUMMARY

DDX5 is a DEAD-box RNA helicase that is overexpressed and implicated in the progression of several cancers, including small cell lung cancer (SCLC). Our laboratory has demonstrated that DDX5 is essential for the invasive growth of SCLC and mitochondrial respiration. SCLC is an extremely lethal, recalcitrant tumor, and currently lacking effective treatments. Supinoxin (RX 5902), a compound having anti-cancer activity, is a known target of phosphor-DDX5. We now report that Supinoxin inhibits the proliferation of chemo-sensitive and chemo-resistant SCLC lines, H69 and H69AR, respectively. Additionally, Supinoxin mitigates both the growth of H69AR xenograft tumors and SCLC PDX tumors *in vivo.* Finally, we find that Supinoxin inhibits expression of mitochondrial genes and effectively blocks respiration. These studies suggest that Supinoxin functions in anti-tumor progression by reducing cellular energy levels through DDX5.

INTRODUCTION

DDX5 belongs to the DEAD-box RNA helicase family, which is the largest class of RNA-dependent helicases in all forms of life.[1] DEAD-box proteins exhibit both RNA-dependent ATPase activity and ATP-dependent helicase activity.[2] These enzymes are involved in all aspects of RNA biology, including transcription, pre-mRNA processing, RNA degradation, and ribosome biogenesis.[2–5] Despite identification of various roles of DEAD-box proteins *in vitro*, specific *in vivo* mechanisms of action for the vast majority of members have remained elusive. Results from our lab have shown that DDX5 exhibits RNA helicase activity *in vitro* and shares functional similarities with its counterpart *DBP2* in *Saccharomyces cerevisiae*.[6] Deleting *DBP2* in *S.cerevisiae* results in significant changes to mRNA secondary structures, which, in turn, affect transcriptional termination.[3] Other studies have also demonstrated that DDX5 regulates alternative splicing through potential secondary structure remodeling.[7,8] Thus, DDX5 and Dbp2 likely remodel RNA secondary structures in nascent RNA during transcription and pre-mRNA maturation phases, contributing to the regulation of gene expression.

DEAD-box family members have been linked to various human diseases, including neurological disorders and cancers.[9,10] DDX5 overexpression has been associated with a range of cancers, such as breast, colon, lung, prostate, and others.[5,9,11–13] DDX5 also serves as a cofactor for oncogenic transcription factors in various cancer types.[13,14] The expression of DDX5 activates the oncogenic Wnt and mammalian target of rapamycin (mTOR) signaling pathways, which play crucial roles in cell-fate determination and cell growth.[15–17] Phosphorylation of DDX5 (pDDX5) at tyrosine 593 (Y593) has been suggested to promote epithelial-mesenchymal transition (EMT) and facilitating the nuclear translocation of β-catenin in colon cancer cell lines.[18,19] Additionally, pDDX5 has been demonstrated to activate the transcription of *Cyclin D1* and *c-Myc*, as well as promote cell proliferation.[20]

Supinoxin, also referred to as RX-5902, is a compound that has been suggested to target pDDX5, with potential anticancer effects.[21,22] These properties were initially discovered during a screening of novel quinoxalinyl-piperazine compounds,[23] which identified RX-5902 (referred to as compound 25).[23] In this study, Supinoxin demonstrated encouraging IC_{50} values in various cancer cell lines, including MDA-MB-231, which is a type of breast adenocarcinoma.[23] Studies conducted in rats showed that Supinoxin has promising bioavailability properties, making it a potential candidate for the development of an anticancer drug.[23,24] It was then found that Supinoxin specifically binds to pDDX5[21] and decreases the expression of *p-c-Jun*, *c-Myc* and *Cyclin D1*.[21,25] It was suggested that Supinoxin acts by interfering with a novel interaction between pDDX5 and β-catenin, resulting in the inhibition of β-catenin nuclear localization and decreased expression of β-catenin-dependent genes.[21] Data

from molecular dynamics simulation assays suggest that Supinoxin binding to pDDX5 could potentially lead to conformational changes in pDDX5 which could preclude binding of β-catenin to pDDX5.[26] A decrease of nuclear β-catenin and the β-catenin-dependent gene MCL-1 has also been shown in upon Supinoxin treatment in triple negative breast cancer (TNBC) cell lines.[22] Moreover, MDA-MB-231 xenograft tumors showed a significant reduction in pDDX5, c-Myc, and β-catenin protein levels after treatment with Supinoxin.[22] Thus, the prevailing model was that Supinoxin interferes with the interaction between pDDX5 and β-catenin, precluding the nuclear translocation of β-catenin and the expression of β-catenin-dependent genes.

Data from our lab shows that DDX5 is upregulated in SCLC, an extremely aggressive and lethal, recalcitrant tumor.[27] Despite being the sixth-most common cause of cancer-related deaths worldwide, the unfortunate reality is that the life expectancy for patients diagnosed with SCLC remains short and treatment options have seen little improvement over the past three decades.[28] The current treatment involves a combination of etoposide/platinum-based chemotherapy and anti-programmed death-ligand 1 (anti-PD-L1) immunotherapy.[29] Sadly, the majority of these patients relapse and only 10–20% survive beyond 2 years, with a median survival time from 7 to 12 months.[22,28,30–32] Previously, our lab showed that DDX5 knockdown reduces proliferation and soft agar colony formation of human SCLC.[27] Furthermore, we found that DDX5 is critical for proper expression of genes required for respiration and mitochondrial functions.[27] Together, these data implicate DDX5 in playing a role in SCLC growth via respiration.

Herein, we show that our previously reported overexpression of DDX5 in SCLC cell lines[27] is due to increased DDX5 protein stability in these cancer cells. Prior studies from other laboratories identified the small molecule Supinoxin (RX-5902) as an inhibitor of tumor progression and further suggested that it acts by inhibiting the nuclear localization and transcriptional function of β-catenin through DDX5.[22] Consistently, we report that Supinoxin is highly effective in inhibiting the growth of SCLC both in *in vitro* SCLC cell lines and *in vivo* mouse models. However, we find that the proposed mechanism of Supinoxin action is incorrect. Rather, we find that Supinoxin inhibits cellular respiration and expression of genes necessary for oxidative phosphorylation, paralleling our prior findings upon knockdown of DDX5.[27] Taken together, these studies suggest that Supinoxin may be an effective chemotherapy with a unique mode of action, providing an entry point for future therapeutic endeavors.

RESULTS

DDX5 protein is more stable in SCLC cell lines

Previous studies conducted in our lab have shown that the levels of DDX5 protein are significantly higher in H69 (chemo sensitive) and H69AR (chemo resistant) cell lines in comparison to the bronchial epithelial cell line HBEC-3KT (HBEC).[27] DDX5 has been found to play a role in the progression of different types of cancers.[15,33,34] We revalidated our prior studies to assess the levels of DDX5 proteins in three cell lines: H69, H69AR, and HBEC-3KT (HBEC). In this study, we utilized a different monoclonal antibody specific to DDX5 for this study, as the level of DDX5 expression in normal lung epithelial HBEC cells was below the detection threshold in our previous report.[27] Consistent with our prior findings, we find that the DDX5 protein is significantly overabundant in SCLC cell lines compared to the noncancerous human bronchial epithelial cell line HBEC-3KT (Figures 1A and 1B). The levels of RFC1 protein were comparable in both SCLC lines and the noncancerous bronchial epithelial cell line HBEC-3KT (Figures 1A and 1B). Previous analysis[35] of 23 clinical small cell lung cancer (SCLC) samples from patients undergoing pulmonary resection revealed that *DDX5* gene expression is actually downregulated in comparison to a normal individual[35] (Figure 1C; data obtained from Gene Expression Omnibus (GEO): GDS4794/225886_at). Similarly, gene expression profiling interactive analysis (GEPIA) (ENSG00000108654) indicates that, except in a few cases such as DLBC, LAML, LGG, THYM cohorts etc., *DDX5* expression is significantly downregulated or has remained at similar levels in almost 62.5% (20 out of 32) of tumor samples and paired normal tissues (Figures 1D and S1).

Consistent with publicly available data, we also found that the levels of *DDX5* transcripts are significantly downregulated in H69 and not statistically different in H69AR SCLC cell lines compared to the noncancerous human bronchial epithelial cell line HBEC-3KT (Figure 1E). Thus, the overabundance of DDX5 protein is not due to increased gene expression. To understand the mechanism, we then measured the relative stability of DDX5 protein using cycloheximide (CHX) chase assays in H69, H69AR, and HBEC-3KT cell lines (Figures 1F–1H). CHX hinders protein synthesis by blocking the elongation phase of protein translation.[36] In comparison to HBEC-3KT, DDX5 is significantly more stable in both H69 and H69AR SCLC cell lines. On the other hand, the relative stability of RFC1 remains comparable across all the cell lines (Figures 1F–1J). Thus, the increased stability of DDX5 protein, rather than the increase in *DDX5* transcripts is responsible for the observed overexpression in SCLC.

Supinoxin inhibits the growth of H69 and H69AR cells

In 2015, the Liu lab discovered the initial link between Supinoxin and DDX5.[21] Through a drug affinity responsive target stability experiment (DARTS) and a filter binding assay, they found that Supinoxin specifically binds to Y593 phosphorylated DDX5 (pDDX5), identifying DDX5 as a cellular target of Supinoxin.[21] Data from our lab shows that, just like triple negative breast cancer cells (TNBC), DDX5 is also upregulated in SCLC.[27] Based on previous studies, we asked whether Supinoxin could potentially be repurposed for treatment of SCLC. To examine the effects of Supinoxin in SCLC, we initially asked if this small molecule could block growth of H69 and/or H69AR by measuring cell proliferation across a range of Supinoxin concentrations. This revealed that Supinoxin inhibits the proliferation of both H69 and H69AR cell lines, with IC_{50} values of 39.81 ± 4.41 nM and 69.38 ± 8.89 nM, respectively (Figures 2A and 2B). Next, we measured the impact of Supinoxin on anchorage-independent growth of SCLC, a hallmark of carcinogenesis, via soft agar colony assays with Supinoxin concentrations at the IC_{50} or without the inhibitor. Interestingly, we found that Supinoxin inhibits colony formation of both H69 and H69AR cells in soft agar (Figures 2B and 2C). Based on these results, we conclude that Supinoxin prevents the growth of H69 and H69AR SCLC cells and hypothesize

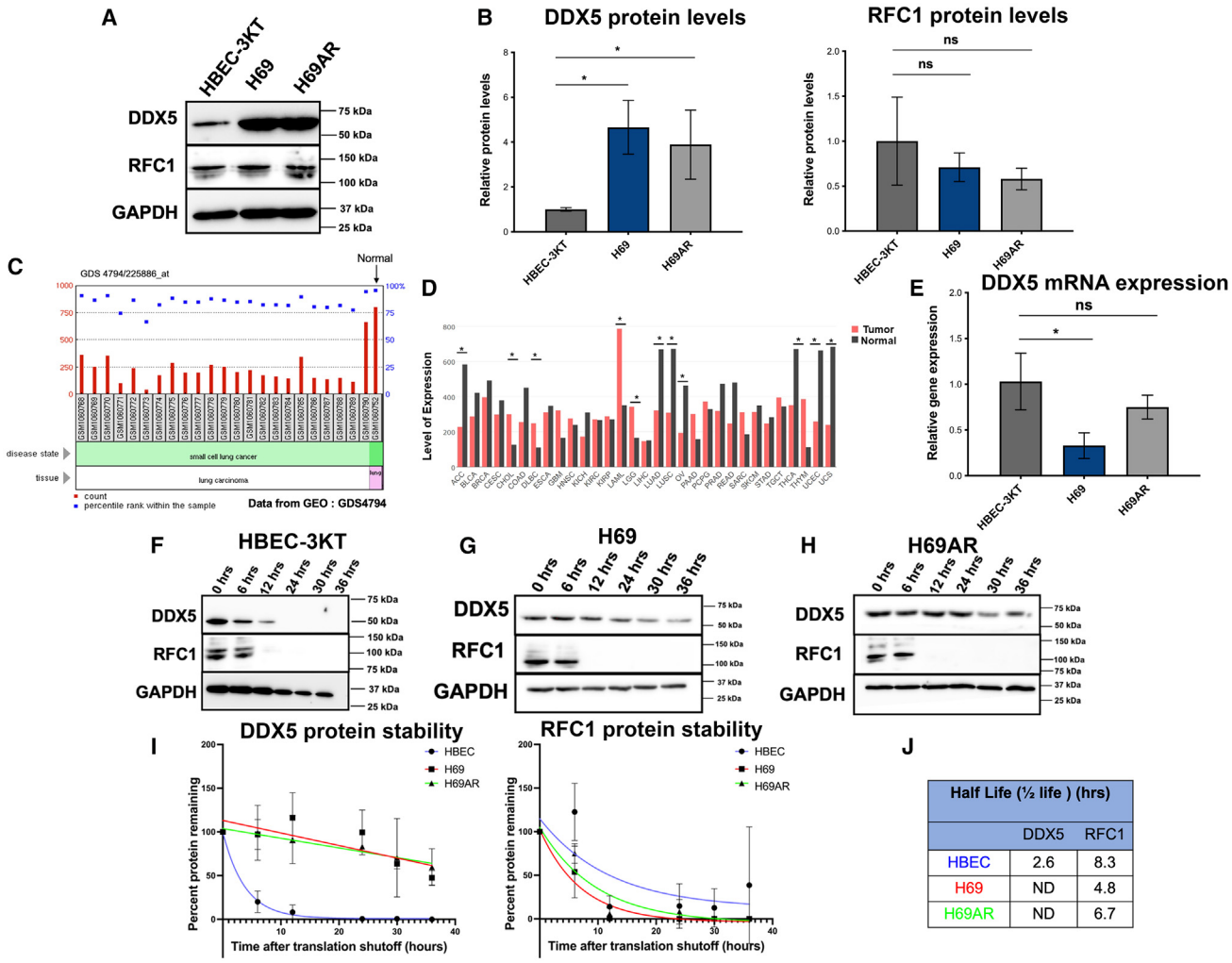

Figure 1. DDX5 protein is more stable in SCLC

(A) Representative western blot images showing the amount of DDX5, RFC1, and GAPDH proteins in HBEC-3KT, H69 and H69AR cells.

(B) Bar graphs depict the quantification of DDX5, RFC1, and GAPDH protein from three different biological replicates in the form of mean ± standard deviation (SD).

(C) *DDX5* gene expression profile of 23 clinical small cell lung cancer (SCLC) samples from patients in comparison to normal lung tissue obtained from Gene Expression Omnibus (GEO): GDS4794/225886_at.

(D) Profile of *DDX5* gene expression across all tumor samples and paired normal tissues from Gene Expression Profiling Interactive Analysis (GEPIA): ENSG00000108654.11. Log_2FC cutoff was set at 1 and the *p* value cutoff was set at 0.01.

(E) RT-qPCR was used to quantify levels of *DDX5* transcripts in HBEC-3KT, H69 and H69AR samples, which were normalized to the expression levels of *GAPDH* mRNA in the form of mean ± standard deviation (SD) from three biological replicates.

(F–H) The stability of DDX5 and RFC1 proteins in HBEC-3KT, H69 and H69AR cells was measured by cycloheximide (CHX) chase assay. RFC1 is a positive control and GAPDH is used as a loading control.

(I and J) Graphical representation of DDX5 and RFC1 protein degradation using the CHX assay. The half-lives were determined from three biological replicates and the signals were normalized to GAPDH. The *p* values are *<0.05, **<0.005, and ***<0.001; ns, not significant.

that it will be an effective antitumor agent against H69AR xenograft and SCLC patient-derived xenograft (PDX) tumors.

Supinoxin inhibits H69AR tumors and SCLC PDX tumors in mice

Next, we investigated the effect of Supinoxin on SCLC *in vivo* to determine if it can reduce the growth of H69AR xenografts. To test this, immunocompromised mice with H69AR xenograft tumors were treated with different concentrations of Supinoxin (17.5, 35, 70 mg/kg) over 25 days. Strikingly, and consistent with *in vitro* studies aforementioned, we observed significant tumor growth inhibition of SCLC tumors in mice with the most striking results observed at a 70 mg/kg dosage (Figure 3A). To test Supinoxin in conditions more representative of cancer patients, we used an SCLC PDX tumor model from Jackson Laboratory (PDX# TM00194). Immunohistochemical (IHC) staining revealed

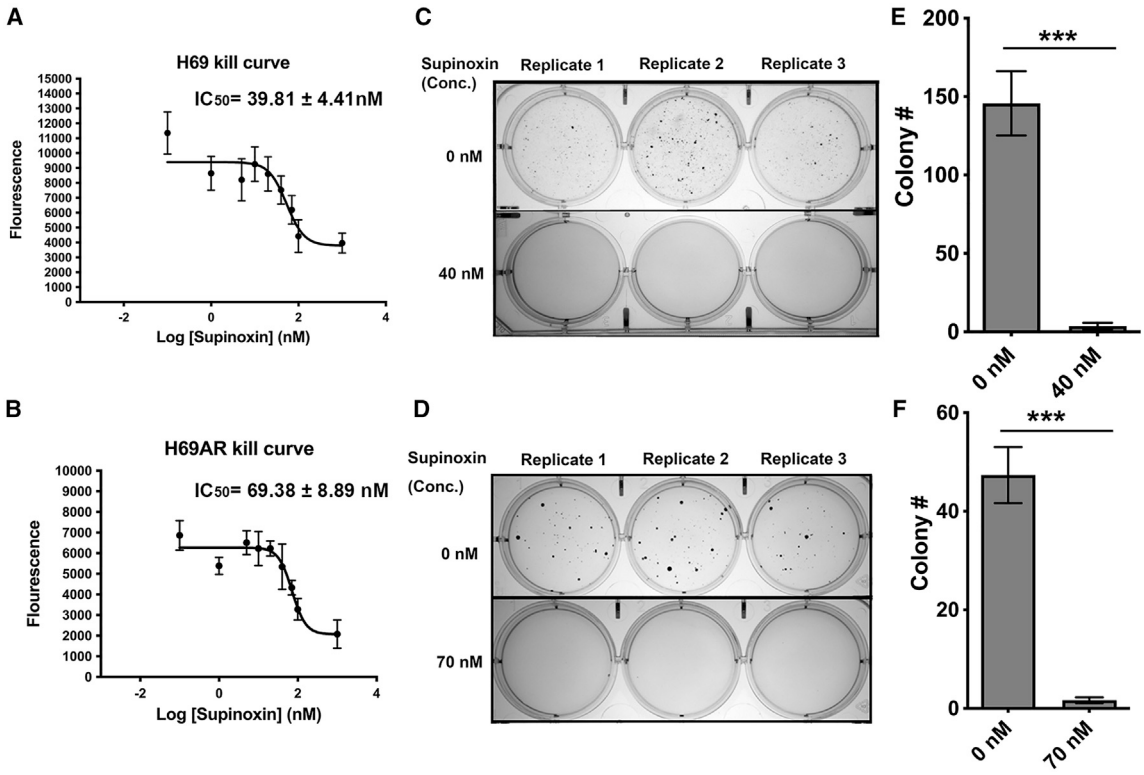

Figure 2. Dose-response curve of Supinoxin in H69 and H69AR cells

(A and B) Varying concentrations of Supinoxin were tested in H69 cells (A) and H69AR cells (B) grown in a 96-well plate for 24 h, after which cell viability was measured using a CyQUANT direct cell proliferation assay Kit. IC_{50} was calculated from three biological replicates.

(C and D) Soft agar colony formation assays were also performed with 0 and 40 nM Supinoxin in H69 cells (C) and 0 and 70 nM Supinoxin in H69AR cells.

(E and F) Quantification of H69 (E) and H69AR (F) soft agar colony assays from three biological replicates in the form of mean ± standard deviation (SD). The *p* values are *<0.05, **<0.005, and ***<0.001; ns, not significant.

a significant upregulation of DDX5 in patient-derived xenograft (PDX) SCLC tumors compared to normal lung tissue (Figures 3B, S2, and S3), consistent with cell line studies. We then tested the effects of Supinoxin on tumor growth in immunocompromised mice with SCLC PDX tumors versus a vehicle-only control. Results showed Supinoxin treatment was sufficient to improve survival (Figure 3C) and inhibit tumor growth (Figure 3D) in a PDX model. We stopped drug treatment after 39 days to see if Supinoxin permanently inhibited tumor growth, however, the tumors resumed growth upon drug removal. This suggests that Supinoxin is effective in tumor growth inhibition, but usage may require combination therapy approaches to prevent relapse.

The expression of c-myc, DDX5, and β-catenin remain unaltered upon treatment Supinoxin

Previous data from other labs suggested that Supinoxin acts by interfering with the interaction of pDDX5 and β-catenin, resulting in decreased expression of β-catenin-dependent genes like *c-Myc*, *Cyclin D1*, etc. responsible for cancer progression in MDA-MB-231, a triple negative breast cancer cell line.[22] We found out that the relative steady state levels of *c-Myc*, *Cyclin-D1*, and *DDX5* transcripts remained significantly unaltered upon Supinoxin treatment in H69AR SCLC cells (Figure 4A). To independently validate previous claims that treatment with Supinoxin decreases the protein levels of β-catenin-dependent genes, we performed Supinoxin treatment on H69AR cells using the same conditions (0, 20, and 70 nM incubation for 24 h) described in Kost et al.[21] However, western blotting showed no significant change in the protein levels of c-Myc, a β-catenin-dependent gene, upon Supinoxin treatment. We also did not observe any significant change in DDX5 or β-catenin protein levels (Figures 4B–4E). We wondered if this difference from prior reports could be due to the tumor type, thus we then analyzed the protein levels of c-Myc, DDX5 and β-catenin upon Supinoxin treatment in MDA-MB-231 cells, the same cell line used in prior studies.[21] Consistent with Supinoxin treatment of SCLC cells, we observed that the transcript levels (Figure 5A) and protein levels (Figures 5B–5E) of c-Myc, DDX5 and β-catenin were unaltered in breast cancer cells.

The localization of β-catenin and pDDX5 are unaffected upon treatment with Supinoxin

Data suggest[21,22,37] that Supinoxin treatment results in a decrease in nuclear β-catenin levels. To test this, we performed immunofluorescence microscopy on MDA-MB-231 and H69AR cells treated for 24 h with (70nM) or without Supinoxin and found no significant difference in nuclear β-catenin localization in both the conditions (Figure 6A). Given that Supinoxin is thought to

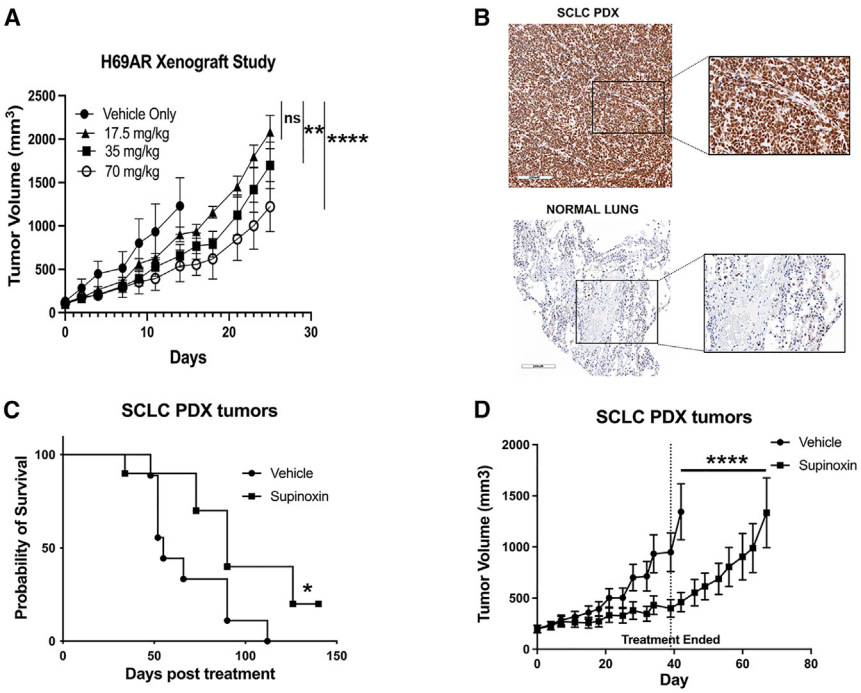

Figure 3. Supinoxin inhibits tumor growth and increases the survival of mice with H69AR-based tumors and patient-derived xenograft (PDX) SCLC tumors

(A) Immunocompromised NOD-Rag1null IL2rgnull (NRG) mice bearing H69AR xenograft tumors were treated with 17.5, 35, or 70 mg/kg Supinoxin or vehicle only for 25 days to identify the best dose for tumor growth inhibition in the absence of significant toxicity based on weight gain. The statistics were calculated using Tukey's multiple comparisons test.

(B) Overexpression of DDX5 in PDX SCLC samples used to generate PDX tumors. Histological staining was performed on SCLC PDX tumors and normal human lung tissues, Scale bar, 200 μm. Images were taken using a Leica DM6 microscope with 10× objective. Brown indicates DDX5 staining.

(C) Immunocompromised NRG mice bearing PDX tumors were administered Supinoxin at 70 mg/kg as a slurry using saline with 10% DMSO as the vehicle. Supinoxin or vehicle was administered for a duration of 8 weeks to assess the survival curve in each group. The statistical evaluation was performed using the log rank Mantel-Cox test. The *p* value is 0.022.

(D) PDX mice were treated with 70 mg/kg Supinoxin or vehicle for 39 days. The data were no longer collected when mice needed to be euthanized. The sample size for mouse experiments is $n = 9$ per group and is representative of 3 independent experiments. Statistical evaluation was performed using the two-way ANOVA test. The *p* values are *<0.05, **<0.005, and ***<0.001; ns, not significant.

specifically target pDDX5[22,26] and that Supinoxin treatment has no effect on DDX5 protein levels, we investigated whether Supinoxin treatment might change the localization of pDDX5 in H69AR and MDA-MB-231 cells. pDDX5 is primarily cytoplasmic, in contrast to the total DDX5, which is predominantly nuclear. However, we did not observe any significant changes in pDDX5 localization in H69AR or MDA-MB-231 cells (Figure 6B). We also investigated the localization of pDDX5 at various time points upon treatment with 100 mM of Supinoxin in MDA-MB-231 cells, in case a response was time-dependent. Again, no significant change in pDDX5 localization was observed (Figure 6C), indicating that DDX5 in our system does not function through the β-catenin pathway as previously thought.[21,22,37]

Mitochondrial functions are downregulated in H69AR cells upon Supinoxin treatment

In order to identify the genes impacted by Supinoxin treatment on a global level, RNA-seq was conducted on H69AR cells treated with or without Supinoxin. We obtained approximately 3×10^7 mapped reads for each of the three biological replicates. The genome mapping for all samples were ~95%. The separation of samples by their group and the localization of samples within groups were then visualized using principal-component analysis (PCA) using DESeq2 and edgeR (Figure S4). We chose to use three replicates of H69AR, both with and without Supinoxin, based on the variance. The PCA algorithm offers a comprehensive analysis of the primary directions of greatest variability in the data, making it suitable for clustering purposes. This successfully identified a significant number of differentially expressed genes (DEGs) upon the addition of Supinoxin with a false discovery rate (FDR) of <0.05. We then compared the list of Supinoxin-responsive genes with our prior RNA-seq data of H69AR cells +/− DDX5 knockdown.[27] This revealed that a total of 433 transcripts (Figure 7A) are significantly downregulated upon both Supinoxin treatment and DDX5 knockdown.[27] The expression patterns of selected genes across treated and untreated samples were then illustrated in a heatmap generated in RStudio (Figure 7B). Genes clustered at the top were found to be predominantly downregulated upon treatment. Statistically significant changes, aiding in the identification of critical molecular players, were then visualized using a volcano plot (Figure 7C).

We then determined the Kyoto Encyclopedia of Genes and Genomes (KEGG) pathways that were altered to investigate the cellular processes impacted by Supinoxin. Pathway analysis and functional annotation for up and downregulated genes were performed using the R software package enrichR and gene set enrichment analysis (GSEA). A total of 1227 genes were found to be upregulated, while 1405 genes were downregulated that mapped to a total of 152 KEGG pathways. Figure 8A displays the top 10 that were enriched. Interestingly, DEGs were closely grouped in a number of pathways, including those involving ribosomal components, oxidative phosphorylation, and cytochrome p450-mediated xenobiotic metabolism, indicating that Supinoxin exerts its effects through the mitochondrial pathway. In our prior study we found mitochondrial dysfunction upon DDX5 knockdown.[27] It is worth noting that Supinoxin treatment as well as DDX5 knockdown resulted in significant alterations in oxidative phosphorylation (OXPHOS) (Figure 8A).[27] Consistently, GSEA analysis showed that oxidative phosphorylation is significantly downregulated with the treatment of Supinoxin.

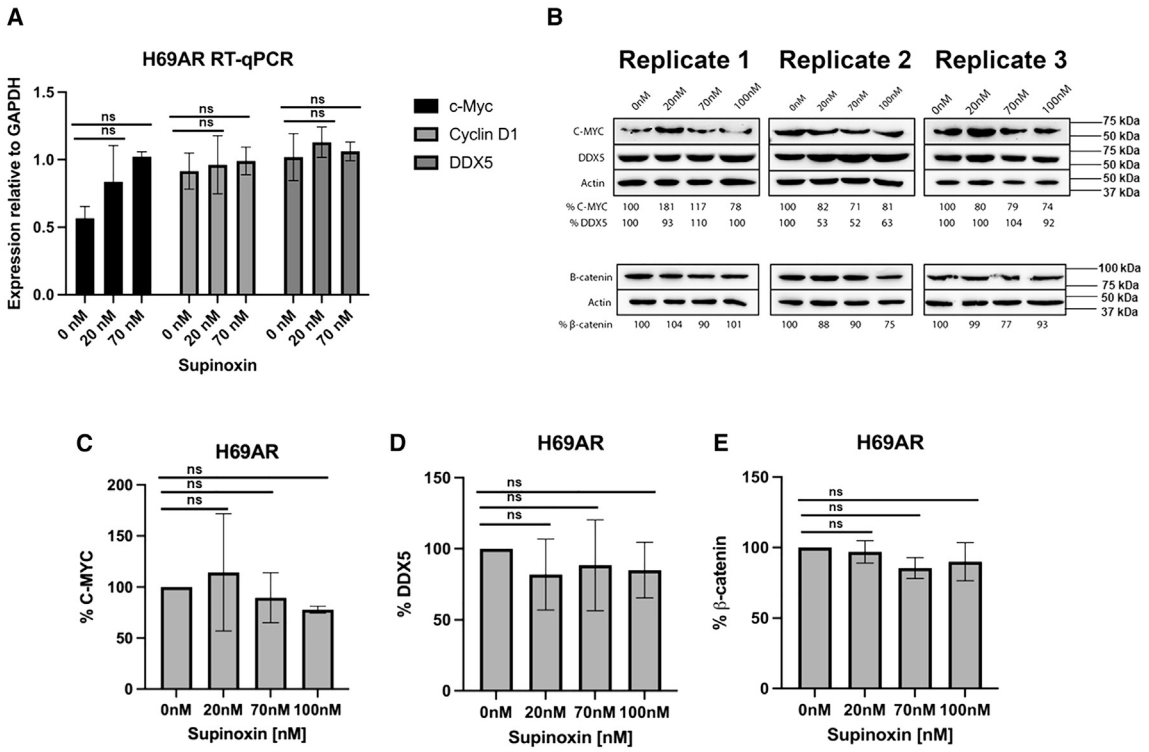

Figure 4. The expression of c-Myc, DDX5 and β-catenin does not change significantly upon treatment with various concentrations of Supinoxin in H69AR cells

(A) RT-qPCR was used to quantify levels of *DDX5*, *Cyclin D1*, and *c-Myc* transcripts, which were normalized to the expression levels of *GAPDH* mRNA in the form of mean ± standard deviation (SD) from three biological replicates.

(B) Representative western blot images showing the amount of c-Myc, DDX5, β-catenin and β-actin proteins following Supinoxin treatment in H69AR cells.

(C–E) Bar graphs depict the quantification of c-Myc, DDX5 and β-catenin proteins from three different biological replicates in the form of mean ± standard deviation (SD). The *p* values are *<0.05, **<0.005, and ***<0.001; ns, not significant.

The OXPHOS pathway appears to be deactivated by Pathview with a *p* value of 0.0021 (Figure 8B). This deactivation is accompanied by the downregulation of 74 genes that are involved in the formation of complex I-V (Figure 8C). Also noteworthy is that oxidative phosphorylation was similarly impacted upon DDX5 knock down in H69AR cells in our previous investigation.[27]

Cellular respiration is compromised in H69AR cells upon Supinoxin treatment

To independently validate our RNA-seq results, we conducted RT-qPCR on select genes (Figure 9A) following Supinoxin treatment. This revealed significant downregulation of the relative steady state levels of *SDHAF3*, *SUCLG1*, *COX5B*, *UQCRH*, *MDH1B*, and *NDUFA1* transcripts, consistent with our RNA-seq analysis. The genes impacted upon Supinoxin treatment are nuclear encoded mitochondrial genes similar to that found in our previous study with DDX5 knockdown.[27] Finally, we evaluated the impact of Supinoxin on the function of mitochondria in H69AR cells. We measured the rate of oxygen consumption (OCR) in H69AR cells treated with and without Supinoxin to assess the rate of mitochondrial respiration. First, we injected oligomycin (1.5 μM)[38] into the assay, which inhibits ATP synthase by reducing the flow of electrons through the electron transport chain (ETC), leading to a decrease in OCR. The reduction in OCR is associated with cellular ATP production. The second injection included FCCP (carbonyl cyanide-p-[trifluoromethoxy] phenylhydrazone) (1 μM), which functions as an uncoupler by facilitating the transport of protons across mitochondrial cell membranes, thereby disrupting ATP synthesis.[39] The FCCP is utilized to assess the maximal respiratory capacity of the cell. The third injection was composed of a mixture of rotenone, which acts as a complex I inhibitor, and antimycin A, which functions as a complex III inhibitor (Rot/AA). Rot/AA (0.5 μM) inhibits mitochondrial respiration and allows for the assessment of nonmitochondrial respiration.[40] This analysis revealed a significant decrease in both basal and maximal oxygen consumption rates following Supinoxin treatment. The spare respiratory capacity is also diminished, indicating a lowered capacity to meet heightened energy demands (Figures 9B and 9C). Taken together, our studies suggest that Supinoxin treatment leads to the suppression of nuclear encoded mitochondrial genes related to oxidative phosphorylation, which in turn causes mitochondrial dysfunction in H69AR SCLC cell lines (Figure 9D).

DISCUSSION

SCLC is a highly aggressive form of lung cancer, accounting for around 15% of all bronchogenic carcinomas, with an estimate of

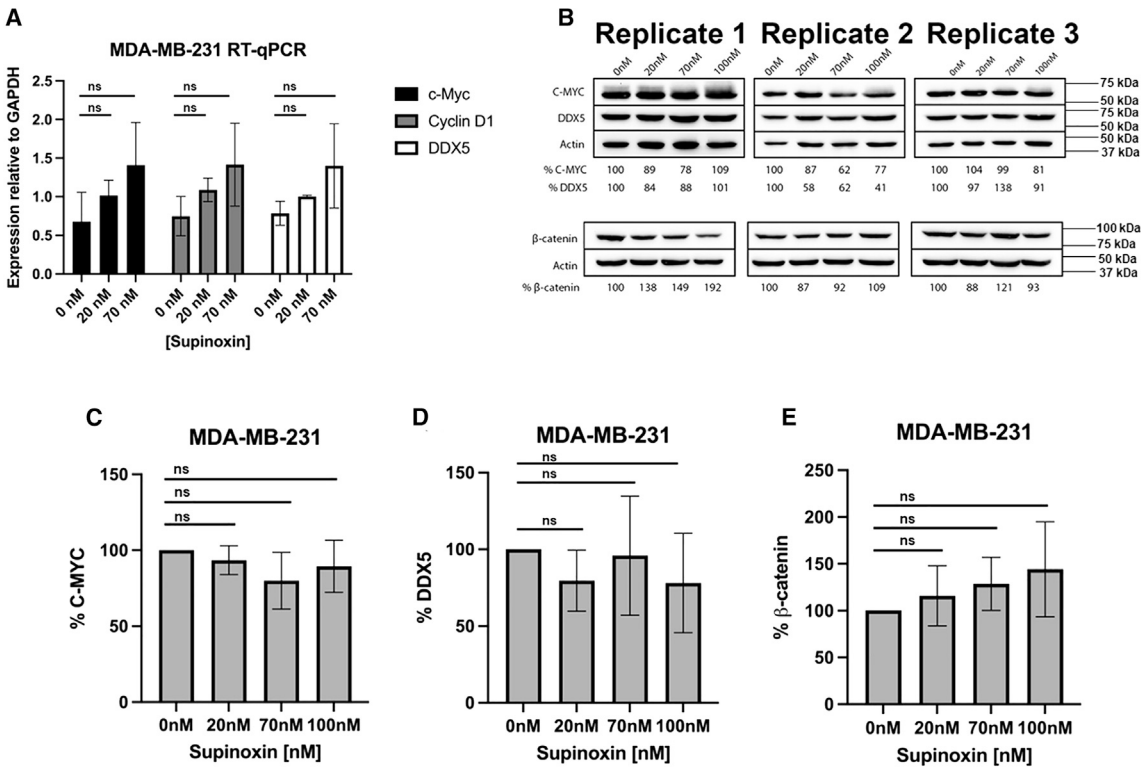

Figure 5. The expression of c-Myc, DDX5 and β-Catenin does not change significantly upon treatment with various concentrations of Supinoxin in MDA-MB-231 cells

(A) RT-qPCR was used to quantify levels of *DDX5*, *Cyclin D1* and *c-Myc* transcripts, which were normalized to the expression levels of GAPDH mRNA in the form of mean ± standard deviation (SD) from three biological replicates.

(B) Representative western blot images showing the amount of c-Myc, DDX5, β-Catenin and β-Actin proteins following Supinoxin treatment in MDA-MB-231 cells.

(C–E) Bar graphs depict the quantification of c-Myc, DDX5 and β-catenin expression from three-four different biological replicates in the form of mean ± standard deviation (SD). The *p* values are *<0.05, **<0.005, and ***<0.001; ns, not significant.

~250,000 new cases diagnosed in the U.S. in 2022 (www.cancer.gov) and is most strongly linked to smoking. It is worth noting that only 2% of cases are found in individuals who have never smoked.[28,41,42] The most common genetic alterations observed in SCLC involve the inactivation of tumor-suppressor genes, *TP53* and *RB1*, in addition to copy-number gains of genes encoding MYC family members, receptor tyrosine kinases and their downstream effectors, chromatin remodeling enzymes, as well as Notch family proteins.[28,43,44] Individuals with lung-confined, localized SCLC cancer without detectable metastases may opt for surgical resection to remove their primary tumor, which has been linked to enhanced survival rates.[30,45–47] Unfortunately, close to 70% of SCLC patients are diagnosed with metastatic disease, frequently with macro-metastases in the brain, liver, lymph nodes, and bones.[30] The median survival rate for patients with SCLC is typically between 7 and 12 months following diagnosis.[30–32,48] Previous studies have shown that SCLC cells tend to spread through the lymphatic system and blood vessels at earlier stages compared to other types of lung cancer cells, making surgical resection less effective.[49,50] As a result, the treatment approach was redirected toward radiation and chemotherapy. However, even though SCLC tumors exhibit a high sensitivity to chemotherapy initially,[50–52] the rapid onset of chemoresistance in SCLC poses a significant challenge for treatment.[53] An etoposide/platinum (EP) combination was widely used as the standard treatment for SCLC until ~5 years ago when the incorporation of anti-programmed death-ligand 1 immunotherapy to EP chemotherapy slightly enhanced survival rates.[50,54–56] In the last three decades, there has been a lack of significant advancements in standard chemotherapy and radiation therapies for SCLC, with the exception of immune checkpoint inhibitors. Unfortunately, these inhibitors prolong survival by only a few months.[30,55,57,58] To combat SCLC, it is crucial to develop highly effective and innovative therapies for treatment.

DEAD-box RNA helicases represent the most abundant category of enzymes within the RNA helicase family. These enzymes function as non-processive, ATP-dependent RNA-binding proteins, exerting their effects on remodeling secondary structures and/or RNA-protein complexes. They play crucial roles in various aspects of RNA biology, including transcription, translation, and RNA decay.[59] Interestingly, increased expression of individual DEAD-box protein family members has been associated with cellular transformation and is found in various types of cancers

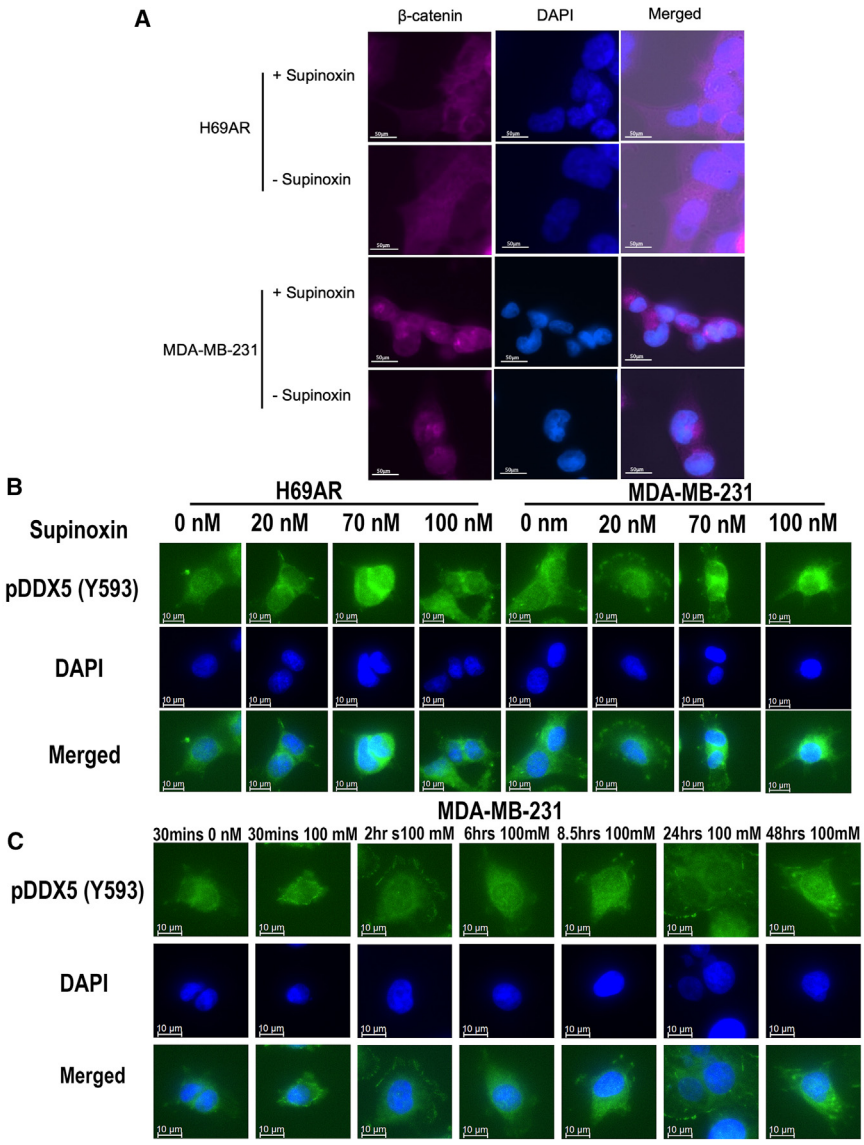

Figure 6. Supinoxin has no effect on the localization of β-catenin or pDDX5 in H69AR or MDA-MB-231 cells

(A) The localization of β-catenin does not change in the presence or absence of Supinoxin in H69AR cells or MDA-MB-231 cells. Cells were seeded onto coverslips and allowed to grow overnight. Supinoxin was then added and incubated on cells for 24 h, after which cells were fixed. The cells were then prepared for immunofluorescence microscopy (IF) to visualize the localization of β-catenin protein, Scale bar, 50 μm. Cells were visualized using Leica DM6 microscope using 40× objective.

(B) The localization of pDDX5 does not change in the presence of various concentrations of Supinoxin in H69AR cells or MDA-MB-231 cells. pDDX5 is shown in green and DAPI in blue, Scale bar, 10 μm.

(C) The localization of pDDX5 does not change in the presence of 100 mM of Supinoxin over time in MDA-MB-231 cells, Scale bar, 10 μm.

such as breast, colon, bone, and prostate cancer.[20,60] DDX5 itself has been implicated in the development of various types of cancers[15,33,34,61,62] and previous studies from our lab showed that the RNA helicase DDX5 plays a crucial role in the invasive growth of SCLC.[27] Knockdown of DDX5 leads to significant defects in mitochondrial respiration through downregulation of nuclear-encoded mitochondrial genes in SCLC, thereby reducing the capacity of these cancer cells to generate the necessary energy to sustain cellular functions.[27] Nuclear DNA-encoded mitochondrial genes play a crucial role in regulating mitochondrial homeostasis through the modulation of mitochondria-related gene expression in cancer cells.[63–66]

Previous investigations from our laboratory demonstrated that the levels of DDX5 protein are significantly elevated in the H69 and H69AR SCLC cell lines,[27] a finding that has been reconfirmed in this study. We have extended this observation by showing that this increase is due to stabilization of DDX5 in SCLC cell lines rather than increased gene expression. Overexpression was also observed in PDX SCLC tumors when compared to normal lung tissue by IHC staining. This finding emphasizes the importance of DDX5 in the development of SCLC. The finding that enhanced protein stability in SCLC accounts for overexpression may solve a puzzle regarding DDX5 and links to cancer, as a multitude of studies have not been able to reconcile DDX5 overabundance with decreased mRNA.[35] Thus, these data extend beyond small cell lung cancer, as *DDX5* mRNA abundance tends to be lower or remained similar in most tumor samples compared to normal tissues (data obtained from Gene Expression Omnibus (GEO): GDS4794/225886_at).

We currently do not know why DDX5 is more stable in SCLC than normal, noncancerous cells or tissues. However, preliminary data from our lab suggests that post-translational modifications may be involved. This may involve the previously reported phosphorylation of Y593 or other post-translational modifications that have been identified on DDX5 including O-GlcNAcylation, sumoylation, and phosphorylation.[21,67,68] Regardless, our studies show the importance of analyzing both the proteome as well as steady-state levels of mRNA to understand the underlying basis of human disease states.

Supinoxin has been shown to abolish the growth and metastasis of TNBC cells both *in vitro* and *in vivo*.[22,23] Studies indicate that treatment with Supinoxin led to apoptosis, G2/M cell-cycle arrest, and aneuploidy in certain breast cancer cell lines.[37] Our studies illustrate the potential of repurposing Supinoxin as a treatment for both chemo sensitive and chemo resistant SCLC. The vast majority of extensive-stage SCLC patients experience

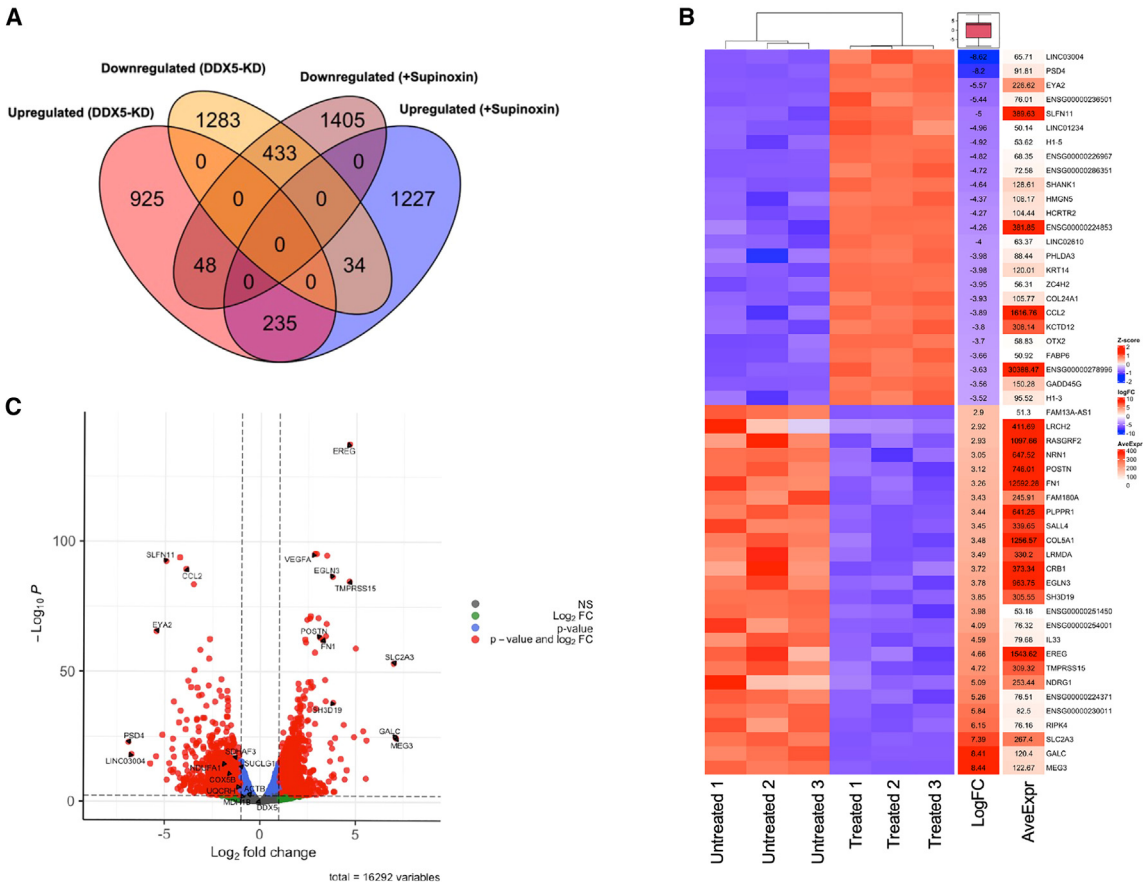

Figure 7. RNA-seq analysis reveals downregulated mitochondrial function following Supinoxin treatment

(A) A Venn diagram illustrating the total number of transcripts upregulated and downregulated following Supinoxin treatment and DDX5 knockdown. It was generated using the Venn diagram package in R Studio (version 2023.12.0).

(B) A heatmap was generated to display the differential expression patterns of transcripts affected by Supinoxin treatment. Red indicates upregulation, while blue represents downregulation, based on Log_2FC values. Z scores were applied to enhance gene clustering in response to Supinoxin treatment. Expression intensity values were calculated using RStudio to analyze gene expression levels.

(C) Volcano plot depicting differentially expressed genes (DEGs) between H69AR cells with or without Supinoxin treatment. The plot was generated from the *p* values (*<0.05, not significant) and Log_2FC values (>1; <−1). The colored dots indicate genes with significant expression differences. Blue dots represent genes with significant differences based on *p* value alone, green dots on Log_2FC alone, red dots represent genes with significant differences based on both *p* value and Log_2FC, and gray dots are not significant in either term.

relapses and develop resistance to initial chemotherapy within a year.[69,70] Immune checkpoint inhibitors have improved the treatment of SCLC. However, due to the significant variability in SCLC, immune checkpoint inhibitors only provided dramatic improvements to a limited subset of patients; overall, the benefits are negligible.[71] Therefore, it is crucial to explore new therapeutic options to combat the chemo resistant SCLC.[70,72] The findings from our study indicate that Supinoxin has the potential to effectively suppress the growth of chemo resistant SCLC cell lines *in vitro*. However, Supinoxin does not completely eradicate the tumor, only slowing or pausing growth in both H69AR and PDX mouse models. This indicates that Supinoxin has a static rather than cytotoxic effect on tumor growth. This is an important observation which suggests that a combination therapy approach involving Supinoxin may be an effective future treatment for SCLC patients.

Another important finding from our studies is that Supinoxin does not function through the currently prevailing model in the field in either SCLC or MDA-MB-231 cells used in prior studies.[21,22] In those studies, there was a decreased expression of β-catenin target genes, while we did not. A previous study[21] used a western blot with no replicates and no quantification. In our study, we have three biological replicates with proper quantification. Moreover, we measured both protein and mRNA levels, the latter of which is more representative of the role of beta-catenin as a transcription factor. We currently cannot explain how prior studies came to this model, as our findings do not indicate any role for β-catenin in the mechanism of Supinoxin. Rather, we find that administration of Supinoxin results in the inhibition of genes associated with oxidative phosphorylation, leading to impaired mitochondrial function in H69AR SCLC cell lines. These findings align with our previous studies

A

Top 10 pathways affected upon Supinoxin treatment

Enrichment Pathways	P-Value
Ribosome	1.01E-14
Oxidative phosphorylation	3.82E-07
Valine, leucine and isoleucine degradation	9.31E-04
Proteasome	1.64E-03
DNA replication	1.85E-03
Pyrimidine metabolism	3.44E-03
Glutathione metabolism	4.97E-03
Tryptophan metabolism	7.68E-03
Peroxisome	8.97E-03
Purine metabolism	9.10E-03

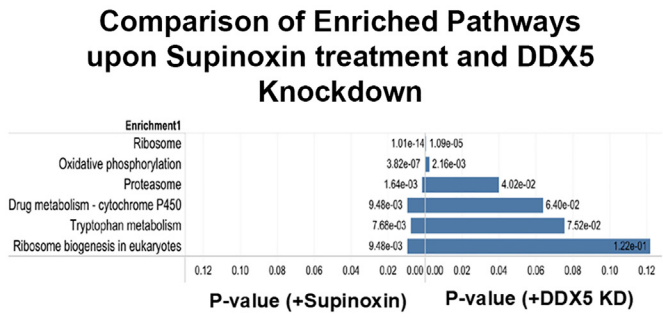

B

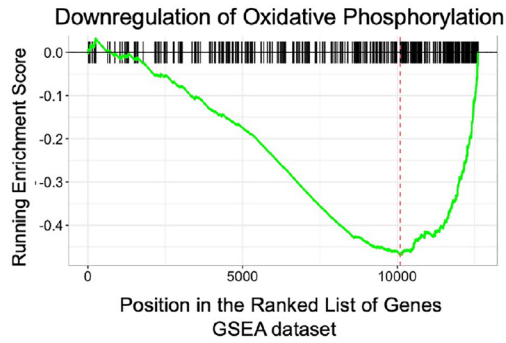

C

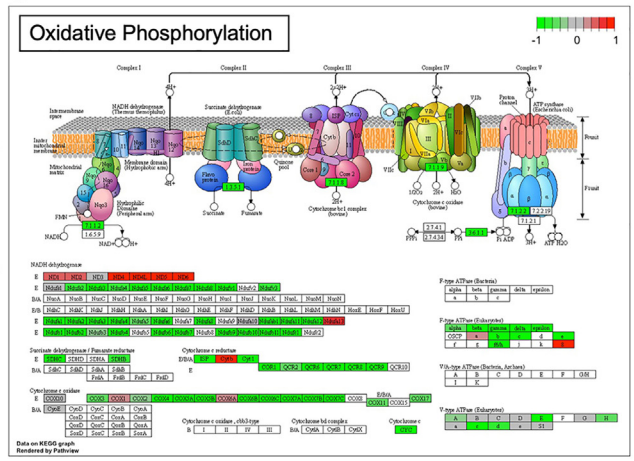

Figure 8. Canonical pathways affected upon Supinoxin treatment

(A) Table showing the top canonical pathways associated with differentially expressed genes (DEGs) upon Supinoxin treatment in H69AR cells, analyzed using DESeq2 and Pathview. A comparison of the enriched pathways was performed upon Supinoxin treatment and DDX5 knockdown. The pathways were analyzed by using the Kyoto Encyclopedia of Genes and Genome (KEGG) pathway analysis.

(B) Gene set enrichment analysis (GSEA) of oxidative phosphorylation pathway genes in H69AR with or without Supinoxin-treatment from KEGG collections.

(C) The Pathview tool was used to analyze the oxidative phosphorylation pathways affected upon Supinoxin treatment. Red indicates high expression and green indicates low expression.

of DDX5.[27] This suggests that SCLC cells exhibit a diminished ability to fulfill increased energy demands when treated with Supinoxin. It is of note that our studies revealed no significant toxic effects of Supinoxin in mice, suggesting specificity for cancerous cells.

The link between upregulation of ATP and cellular building block generation has been well established for decades as a hallmark of cancers.[73–76] Several recent investigations have shown that oxidative phosphorylation (OXPHOS) is increased in different types of cancers, which could make them more susceptible toward its inhibition. In addition, OXPHOS inhibition has been demonstrated to decrease the oxygen consumption rate which can help alleviate tumor hypoxia.[77–79] In addition, research findings indicate that lung tumors possess a high level of oxidative activity, and that lung cancer development relies on OXPHOS.[77–80] Interestingly, mitochondrial respiration and OXPHOS are regulated by apoptosis-inducing factor, which plays a role in the advancement of non-small cell lung cancer.[79]

Multiple reports indicate that cancer stem cells (CSCs) also heavily depend on oxidative phosphorylation (OXPHOS) rather than glycolysis.[81–84] In a study conducted by Lagadinou et al.,[83] it was found that leukemia CSCs exhibited a higher dependence on OXPHOS for their energy supply. It was proposed that inhibiting oxidative phosphorylation could effectively eliminate CSCs in the H446 small cell lung cancer cell line.[84] Interestingly, we observed a decrease in *Cytochrome c oxidase subunit 5B* (*COX5B*) transcripts following Supinoxin treatment. It has been reported that COX5B could potentially play a significant role in predicting the prognosis of breast cancer.[85] Reducing the expression of COX5B in breast cancer cell lines have been found to inhibit cell growth and trigger cell senescence, resulting in an increase in the production of IL-8 and other cytokines.[86] Developing more effective therapeutic options requires a deeper understanding of the molecular mechanisms involved in the initiation, cellular transformation, progression, and establishment of SCLC chemoresistance.

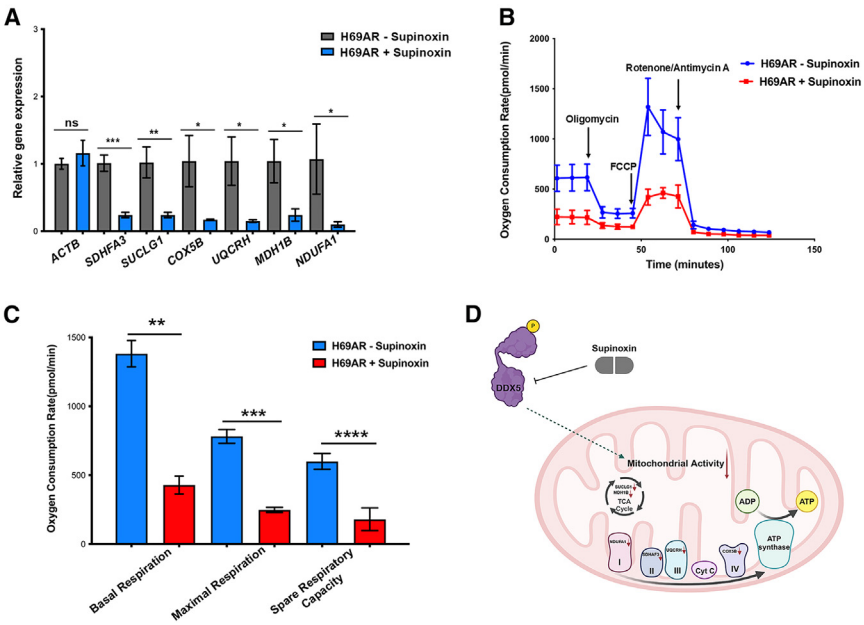

Figure 9. Supinoxin induces mitochondrial dysfunction in SCLC

(A) RT-qPCR was used to quantify levels of *ACTB*, *SDHAF3*, *SUCLG1*, *COX5B*, *UQCRH*, *MDH1B*, and *NDUFA1* transcripts, which were normalized to the expression levels of GAPDH mRNA in the form of mean ± standard deviation (SD) from three biological replicates.

(B and C) Oxygen consumption rates of H69AR cells with or without Supinoxin were measured using the Seahorse XFe24 metabolic flux analyzer. The data represents the mean ± standard deviation (SD) of three biological replicates. The *p* values are *<0.05, **<0.005, and ***<0.001; ns, not significant.

(D) Model depicting the mechanism of Supinoxin in SCLC. Supinoxin interacts with DDX5, and down-regulates nuclear-encoded mitochondrial genes involved in oxidative phosphorylation, leading to mitochondrial dysfunction in SCLC. This suggests that Supinoxin acts through DDX5 by inhibiting an as-of-yet unknown role for this enzyme in promoting cellular respiration in SCLC.

SCLC is commonly diagnosed through fine needle aspiration. However, conducting biopsies upon relapse is not a standard practice. Additionally, obtaining research biopsies poses challenges because of the rapid progression of this cancer type and the presence of patient comorbidities.[87] While SCLC PDX models can be difficult to establish, it is possible to generate SCLC PDX lines in settings where a well-established clinical-translational pipeline for tissue collection is available. Additionally, organoids can be generated for PDX creation via an automated microfluidic system for the enrichment of circulating tumor cells (CTCs).[88] However, these methods are not widely available to most researchers. As a result, many reports use small numbers of PDX due to these difficulties.[89] Our report uses two human SCLC tumor models, the H69AR cell line and the TM00194 PDX cell line. While our data demonstrates remarkable similarities between the two, the formal argument exists that the data do not account for potential variability and tumor heterogeneity between patients. This is certainly a caveat; however, our investigation holds significant value not only for future treatment of SCLC but also for targeted therapies across various types of cancers. Moreover, our studies illustrate that exploration of RNA biology can lead to potential new targets for human disease intervention.

Limitations of the study

In this study, we utilized two human SCLC tumor models: the H69AR cell line and the TM00194 PDX cell line. Although our data reveal remarkable similarities between the two, there is a formal argument that the data do not account for potential variability and tumor heterogeneity among patients. Additionally, we did not independently confirm the binding of Supinoxin to DDX5; however, our RNA-sequencing data from both DDX5 knockdown and Supinoxin treatment indicates that Supinoxin acts through DDX5, resulting in mitochondrial dysfunction in SCLC.

RESOURCE AVAILABILITY

Lead contact

Further information and requests for resources and reagents should be directed to Elizabeth J. Tran (ejtran@purdue.edu).

Materials availability

This study did not generate new unique reagents.

Data and code availability

- RNA-seq data have been deposited in the NCBI Gene Expression Omnibus database and are publicly available as of the date of publication. The accession number (GEO Database: GSE255741) is listed in the key resources table.
- Original western blot images have been deposited at Mendeley at Mendeley Data (V1): https://doi.org/10.17632/r6ryb6ckps.1 and are publicly available as of the date of publication. Microscopy data reported in this paper will be shared by the lead contact upon request.
- This article does not report any original code.
- Any additional information required to reanalyze the data reported in this paper is available from the lead contact upon request.

ACKNOWLEDGMENTS

This work was supported by funding from the Purdue University Institute for Cancer Research to E.J.T. and B.D.E. and National Institutes of Health grants P30CA023168 and P30CA082709 for Collaborative Core for Cancer Bioinformatics and Biological Evaluation Shared Resource at the Purdue University Institute for Cancer Research and Indiana University Simon Cancer Center, the Walther Cancer Foundation, Indianapolis, IN. We are grateful to all our collaborators for all the insightful comments and suggestions that have contributed to enhancing the quality of the manuscript. The Graphical Abstract, Figures 3B and 9D were created using Biorender.com.

AUTHOR CONTRIBUTIONS

S.D., M.P.R., B.D.E., and E.J.T. conceptualization; S.D., M.P.Z., and M.P.R. data curation; S.D., M.P.R., Z.X., and M.P.Z. validation; S.D., M.P.R., M.P.Z., Z.X., and B.D.E. investigation; S.D., M.P.R., M.P.Z., and B.D.E. methodology; S.D., M.P.R., S.T.-A., H.E.C., H.A.H., and B.D.E. mouse studies;

S.D., M.P.R., M.P.Z., and B.D.E. writing original draft; S.D. and E.J.T. writing and editing; E.J.T. and B.D.E. supervision; E.J.T. and B.D.E. funding acquisition.

DECLARATION OF INTERESTS

The authors declare no competing interests.

STAR★METHODS

Detailed methods are provided in the online version of this paper and include the following:

- KEY RESOURCES TABLE
- EXPERIMENTAL MODEL AND STUDY PARTICIPANT DETAILS
  - Cell lines
  - Animal experiments
  - Ethics committee approval
- METHOD DETAILS
  - Growth analysis
  - RT-qPCR
  - Western Blot
  - Microscopy
  - Histological staining
  - RNA-seq and data analysis
  - Seahorse assay
- QUANTIFICATION AND STATISTICAL ANALYSIS

SUPPLEMENTAL INFORMATION

Supplemental information can be found online at https://doi.org/10.1016/j.isci.2025.112219.

Received: August 7, 2024
Revised: December 26, 2024
Accepted: March 11, 2025
Published: March 13, 2025

REFERENCES

1. Bourgeois, C.F., Mortreux, F., and Auboeuf, D. (2016). The multiple functions of RNA helicases as drivers and regulators of gene expression. Nat. Rev. Mol. Cell Biol. *17*, 426–438. https://doi.org/10.1038/nrm.2016.50.
2. Linder, P., and Jankowsky, E. (2011). From unwinding to clamping — the DEAD box RNA helicase family. Nat. Rev. Mol. Cell Biol. *12*, 505–516. https://doi.org/10.1038/nrm3154.
3. Lai, Y.-H., Choudhary, K., Cloutier, S.C., Xing, Z., Aviran, S., and Tran, E.J. (2019). Genome-Wide Discovery of DEAD-Box RNA Helicase Targets Reveals RNA Structural Remodeling in Transcription Termination. Genetics *212*, 153–174. https://doi.org/10.1534/genetics.119.302058.
4. Putnam, A.A., and Jankowsky, E. (2013). DEAD-box helicases as integrators of RNA, nucleotide and protein binding. Biochim. Biophys. Acta *1829*, 884–893. https://doi.org/10.1016/j.bbagrm.2013.02.002.
5. Xing, Z., Ma, W.K., and Tran, E.J. (2019). The DDX5/Dbp2 subfamily of DEAD-box RNA helicases. WIREs RNA *10*, e1519. https://doi.org/10.1002/wrna.1519.
6. Xing, Z., Wang, S., and Tran, E.J. (2017). Characterization of the mammalian DEAD-box protein DDX5 reveals functional conservation with *S. cerevisiae* ortholog Dbp2 in transcriptional control and glucose metabolism. RNA *23*, 1125–1138. https://doi.org/10.1261/rna.060335.116.
7. Kar, A., Fushimi, K., Zhou, X., Ray, P., Shi, C., Chen, X., Liu, Z., Chen, S., and Wu, J.Y. (2011). RNA Helicase p68 (DDX5) Regulates *tau* Exon 10 Splicing by Modulating a Stem-Loop Structure at the 5′ Splice Site. Mol. Cell Biol. *31*, 1812–1821. https://doi.org/10.1128/MCB.01149-10.
8. Lee, Y.J., Wang, Q., and Rio, D.C. (2018). Coordinate regulation of alternative pre-mRNA splicing events by the human RNA chaperone proteins hnRNPA1 and DDX5. Genes Dev. *32*, 1060–1074. https://doi.org/10.1101/gad.316034.118.
9. Fuller-Pace, F.V. (2013). DEAD box RNA helicase functions in cancer. RNA Biol. *10*, 121–132. https://doi.org/10.4161/rna.23312.
10. Anthony, K., and Gallo, J.-M. (2010). Aberrant RNA processing events in neurological disorders. Brain Res. *1338*, 67–77. https://doi.org/10.1016/j.brainres.2010.03.008.
11. Hashemi, V., Masjedi, A., Hazhir-karzar, B., Tanomand, A., Shotorbani, S.S., Hojjat-Farsangi, M., Ghalamfarsa, G., Azizi, G., Anvari, E., Baradaran, B., and Jadidi-Niaragh, F. (2019). The role of DEAD-box RNA helicase p68 (DDX5) in the development and treatment of breast cancer. J. Cell. Physiol. *234*, 5478–5487. https://doi.org/10.1002/jcp.26912.
12. Shin, S., Rossow, K.L., Grande, J.P., and Janknecht, R. (2007). Involvement of RNA Helicases p68 and p72 in Colon Cancer. Cancer Res. *67*, 7572–7578. https://doi.org/10.1158/0008-5472.CAN-06-4652.
13. Clark, E.L., Coulson, A., Dalgliesh, C., Rajan, P., Nicol, S.M., Fleming, S., Heer, R., Gaughan, L., Leung, H.Y., Elliott, D.J., et al. (2008). The RNA Helicase p68 Is a Novel Androgen Receptor Coactivator Involved in Splicing and Is Overexpressed in Prostate Cancer. Cancer Res. *68*, 7938–7946. https://doi.org/10.1158/0008-5472.CAN-08-0932.
14. Wortham, N.C., Ahamed, E., Nicol, S.M., Thomas, R.S., Periyasamy, M., Jiang, J., Ochocka, A.M., Shousha, S., Huson, L., Bray, S.E., et al. (2009). The DEAD-box protein p72 regulates ERα-/oestrogen-dependent transcription and cell growth, and is associated with improved survival in ERα-positive breast cancer. Oncogene *28*, 4053–4064. https://doi.org/10.1038/onc.2009.261.
15. Du, C., Li, D.Q., Li, N., Chen, L., Li, S.S., Yang, Y., Hou, M.X., Xie, M.J., and Zheng, Z.D. (2017). DDX5 promotes gastric cancer cell proliferation in vitro and in vivo through mTOR signaling pathway. Sci. Rep. *7*, 42876. https://doi.org/10.1038/srep42876.
16. Yang, L., Lin, C., and Liu, Z.-R. (2006). P68 RNA Helicase Mediates PDGF-Induced Epithelial Mesenchymal Transition by Displacing Axin from β-Catenin. Cell *127*, 139–155. https://doi.org/10.1016/j.cell.2006.08.036.
17. Arun, G., Akhade, V.S., Donakonda, S., and Rao, M.R.S. (2012). mrhl RNA, a Long Noncoding RNA, Negatively Regulates Wnt Signaling through Its Protein Partner Ddx5/p68 in Mouse Spermatogonial Cells. Mol. Cell Biol. *32*, 3140–3152. https://doi.org/10.1128/MCB.00006-12.
18. Carter, C.L., Lin, C., Liu, C.-Y., Yang, L., and Liu, Z.-R. (2010). Phosphorylated p68 RNA helicase activates snail1 transcription by promoting HDAC1 dissociation from the snail1 promoter. Oncogene *29*, 5427–5436. https://doi.org/10.1038/onc.2010.276.
19. He, X. (2006). Unwinding a Path to Nuclear β-Catenin. Cell *127*, 40–42. https://doi.org/10.1016/j.cell.2006.09.016.
20. Fuller-Pace, F.V. (2013). The DEAD box proteins DDX5 (p68) and DDX17 (p72): Multi-tasking transcriptional regulators. Biochim. Biophys. Acta *1829*, 756–763. https://doi.org/10.1016/j.bbagrm.2013.03.004.
21. Kost, G.C., Yang, M.Y., Li, L., Zhang, Y., Liu, C.Y., Kim, D.J., Ahn, C.-H., Lee, Y.B., and Liu, Z.-R. (2015). A Novel Anti-Cancer Agent, 1-(3,5-Dimethoxyphenyl)-4-[(6-Fluoro-2-Methoxyquinoxalin-3-yl) Aminocarbonyl] Piperazine (RX-5902), Interferes With β-Catenin Function Through Y593 Phospho-p68 RNA Helicase. J. Cell. Biochem. *116*, 1595–1601. https://doi.org/10.1002/jcb.25113.
22. Capasso, A., Bagby, S.M., Dailey, K.L., Currimjee, N., Yacob, B.W., Ionkina, A., Frank, J.G., Kim, D.J., George, C., Lee, Y.B., et al. (2019). First-in-Class Phosphorylated-p68 Inhibitor RX-5902 Inhibits β-Catenin Signaling and Demonstrates Antitumor Activity in Triple-Negative Breast Cancer. Mol. Cancer Therapeut. *18*, 1916–1925. https://doi.org/10.1158/1535-7163.MCT-18-1334.
23. Lee, Y.B., Gong, Y.-D., Yoon, H., Ahn, C.-H., Jeon, M.-K., and Kong, J.-Y. (2010). Synthesis and anticancer activity of new 1-[(5 or 6-substituted 2-alkoxyquinoxalin-3-yl)aminocarbonyl]-4-(hetero)arylpiperazine derivatives.

Bioorg. Med. Chem. *18*, 7966–7974. https://doi.org/10.1016/j.bmc.2010.09.028.

24. Song, Y.-K., Seol, Y.-H., Kim, M.J., Jeong, J.-W., Choi, H.-I., Lee, S.-W., Chae, Y.-J., Ahn, S., Gong, Y.-D., Lee, K.-R., and Koo, T.S. (2021). Pharmacokinetic Characterization of Supinoxin and Its Physiologically Based Pharmacokinetic Modeling in Rats. Pharmaceutics *13*, 373. https://doi.org/10.3390/pharmaceutics13030373.

25. Yang, L., Lin, C., Zhao, S., Wang, H., and Liu, Z.-R. (2007). Phosphorylation of p68 RNA Helicase Plays a Role in Platelet-derived Growth Factor-induced Cell Proliferation by Up-regulating Cyclin D1 and c-Myc Expression. J. Biol. Chem. *282*, 16811–16819. https://doi.org/10.1074/jbc.M610488200.

26. Ali, W., Shafique, S., and Rashid, S. (2018). Structural characterization of β-catenin and RX-5902 binding to phospho-p68 RNA helicase by molecular dynamics simulation. Prog. Biophys. Mol. Biol. *140*, 79–89. https://doi.org/10.1016/j.pbiomolbio.2018.04.011.

27. Xing, Z., Russon, M.P., Utturkar, S.M., and Tran, E.J. (2020). The RNA helicase DDX5 supports mitochondrial function in small cell lung cancer. J. Biol. Chem. *295*, 8988–8998. https://doi.org/10.1074/jbc.RA120.012600.

28. Sabari, J.K., Lok, B.H., Laird, J.H., Poirier, J.T., and Rudin, C.M. (2017). Unravelling the biology of SCLC: implications for therapy. Nat. Rev. Clin. Oncol. *14*, 549–561. https://doi.org/10.1038/nrclinonc.2017.71.

29. Patel, S.R., and Das, M. (2023). Small Cell Lung Cancer: Emerging Targets and Strategies for Precision Therapy. Cancers *15*, 4016. https://doi.org/10.3390/cancers15164016.

30. Ko, J., Winslow, M.M., and Sage, J. (2021). Mechanisms of small cell lung cancer metastasis. EMBO Mol. Med. *13*, e13122. https://doi.org/10.15252/emmm.202013122.

31. de Castro Carpeño, J., Dols, M.C., Gomez, M.D., Gracia, P.R., Crama, L., and Campelo, M.R.G. (2019). Survival outcomes in stage IV small-cell lung cancer (IV-SCLC): Analysis from SEER database. Ann. Oncol. *30*, xi30. https://doi.org/10.1093/annonc/mdz449.038.

32. Chung, H.C., Piha-Paul, S.A., Lopez-Martin, J., Schellens, J.H.M., Kao, S., Miller, W.H., Delord, J.-P., Gao, B., Planchard, D., Gottfried, M., et al. (2020). Pembrolizumab After Two or More Lines of Previous Therapy in Patients With Recurrent or Metastatic SCLC: Results From the KEYNOTE-028 and KEYNOTE-158 Studies. J. Thorac. Oncol. *15*, 618–627. https://doi.org/10.1016/j.jtho.2019.12.109.

33. Mazurek, A., Luo, W., Krasnitz, A., Hicks, J., Powers, R.S., and Stillman, B. (2012). DDX5 Regulates DNA Replication and Is Required for Cell Proliferation in a Subset of Breast Cancer Cells. Cancer Discov. *2*, 812–825. https://doi.org/10.1158/2159-8290.CD-12-0116.

34. Zhang, M., Weng, W., Zhang, Q., Wu, Y., Ni, S., Tan, C., Xu, M., Sun, H., Liu, C., Wei, P., and Du, X. (2018). The lncRNA NEAT1 activates Wnt/β-catenin signaling and promotes colorectal cancer progression via interacting with DDX5. J. Hematol. Oncol. *11*, 113. https://doi.org/10.1186/s13045-018-0656-7.

35. Sato, T., Kaneda, A., Tsuji, S., Isagawa, T., Yamamoto, S., Fujita, T., Yamanaka, R., Tanaka, Y., Nukiwa, T., Marquez, V.E., et al. (2013). PRC2 overexpression and PRC2-target gene repression relating to poorer prognosis in small cell lung cancer. Sci. Rep. *3*, 1911. https://doi.org/10.1038/srep01911.

36. Schneider-Poetsch, T., Ju, J., Eyler, D.E., Dang, Y., Bhat, S., Merrick, W.C., Green, R., Shen, B., and Liu, J.O. (2010). Inhibition of eukaryotic translation elongation by cycloheximide and lactimidomycin. Nat. Chem. Biol. *6*, 209–217. https://doi.org/10.1038/nchembio.304.

37. Tentler, J.J., Lang, J., Capasso, A., Kim, D.J., Benaim, E., Lee, Y.B., Eisen, A., Bagby, S.M., Hartman, S.J., Yacob, B.W., et al. (2020). RX-5902, a novel β-catenin modulator, potentiates the efficacy of immune checkpoint inhibitors in preclinical models of triple-negative breast Cancer. BMC Cancer *20*, 1063. https://doi.org/10.1186/s12885-020-07500-1.

38. Hao, W., Chang, C.-P.B., Tsao, C.-C., and Xu, J. (2010). Oligomycin-induced Bioenergetic Adaptation in Cancer Cells with Heterogeneous Bioenergetic Organization. J. Biol. Chem. *285*, 12647–12654. https://doi.org/10.1074/jbc.M109.084194.

39. Park, K.-S., Jo, I., Pak, K., Bae, S.-W., Rhim, H., Suh, S.-H., Park, J., Zhu, H., So, I., and Kim, K.W. (2002). FCCP depolarizes plasma membrane potential by activating proton and Na+ currents in bovine aortic endothelial cells. Pflügers Archiv. *443*, 344–352. https://doi.org/10.1007/s004240100703.

40. Yoo, I., Ahn, I., Lee, J., and Lee, N. (2024). Extracellular flux assay (Seahorse assay): Diverse applications in metabolic research across biological disciplines. Mol. Cells *47*, 100095. https://doi.org/10.1016/j.mocell.2024.100095.

41. Pesch, B., Kendzia, B., Gustavsson, P., Jöckel, K.H., Johnen, G., Pohlabeln, H., Olsson, A., Ahrens, W., Gross, I.M., Brüske, I., et al. (2012). Cigarette smoking and lung cancer—relative risk estimates for the major histological types from a pooled analysis of case–control studies. Int. J. Cancer *131*, 1210–1219. https://doi.org/10.1002/ijc.27339.

42. Varghese, A.M., Zakowski, M.F., Yu, H.A., Won, H.H., Riely, G.J., Krug, L.M., Kris, M.G., Rekhtman, N., Ladanyi, M., Wang, L., et al. (2014). Small-Cell Lung Cancers in Patients Who Never Smoked Cigarettes. J. Thorac. Oncol. *9*, 892–896. https://doi.org/10.1097/JTO.0000000000000142.

43. George, J., Lim, J.S., Jang, S.J., Cun, Y., Ozretić, L., Kong, G., Leenders, F., Lu, X., Fernández-Cuesta, L., Bosco, G., et al. (2015). Comprehensive genomic profiles of small cell lung cancer. Nature *524*, 47–53. https://doi.org/10.1038/nature14664.

44. Rudin, C.M., Durinck, S., Stawiski, E.W., Poirier, J.T., Modrusan, Z., Shames, D.S., Bergbower, E.A., Guan, Y., Shin, J., Guillory, J., et al. (2012). Comprehensive genomic analysis identifies SOX2 as a frequently amplified gene in small-cell lung cancer. Nat. Genet. *44*, 1111–1116. https://doi.org/10.1038/ng.2405.

45. Weksler, B., Nason, K.S., Shende, M., Landreneau, R.J., and Pennathur, A. (2012). Surgical Resection Should Be Considered for Stage I and II Small Cell Carcinoma of the Lung. Ann. Thorac. Surg. *94*, 889–893. https://doi.org/10.1016/j.athoracsur.2012.01.015.

46. Barnes, H., See, K., Barnett, S., and Manser, R. (2015). Surgery for localised small cell lung cancer. In Cochrane Database of Systematic Reviews, H. Barnes, ed. (John Wiley & Sons, Ltd). https://doi.org/10.1002/14651858.CD011917.

47. Wang, Y., Zheng, Q., Jia, B., An, T., Zhao, J., Wu, M., Zhuo, M., Li, J., Zhong, J., Chen, H., et al. (2020). Effects of Surgery on Survival of Early-Stage Patients With SCLC: Propensity Score Analysis and Nomogram Construction in SEER Database. Front. Oncol. *10*, 626. https://doi.org/10.3389/fonc.2020.00626.

48. Byers, L.A., and Rudin, C.M. (2015). Small cell lung cancer: Where do we go from here? Cancer *121*, 664–672. https://doi.org/10.1002/cncr.29098.

49. Matthews, M.J., Kanhouwa, S., Pickren, J., and Robinette, D. (1973). Frequency of residual and metastatic tumor in patients undergoing curative surgical resection for lung cancer. Cancer Chemother. Rep. *4*, 63–67.

50. Megyesfalvi, Z., Gay, C.M., Popper, H., Pirker, R., Ostoros, G., Heeke, S., Lang, C., Hoetzenecker, K., Schwendenwein, A., Boettiger, K., et al. (2023). Clinical insights into small cell lung cancer: Tumor heterogeneity, diagnosis, therapy, and future directions. CA Cancer J. Clin. *73*, 620–652. https://doi.org/10.3322/caac.21785.

51. Skarlos, D.V., Samantas, E., Kosmidis, P., Fountzilas, G., Angelidou, M., Palamidas, P., Mylonakis, N., Provata, A., Papadakis, E., Klouvas, G., et al. (1994). Randomized comparison of etoposide-cisplatin vs. etoposide-carboplatin and irradiation in small-cell lung cancer. Ann. Oncol. *5*, 601–607. https://doi.org/10.1093/oxfordjournals.annonc.a058931.

52. Karim, S.M., and Zekri, J. (2012). Chemotherapy for small cell lung cancer: a comprehensive review. Onco Rev. *6*, 4. https://doi.org/10.4081/oncol.2012.e4.

53. Rudin, C.M., and Poirier, J.T. (2017). Shining light on novel targets and therapies. Nat. Rev. Clin. Oncol. *14*, 75–76. https://doi.org/10.1038/nrclinonc.2016.203.

54. Ragavan, M., and Das, M. (2020). Systemic Therapy of Extensive Stage Small Cell Lung Cancer in the Era of Immunotherapy. Curr. Treat. Options Oncol. *21*, 64. https://doi.org/10.1007/s11864-020-00762-8.

55. Horn, L., Mansfield, A.S., Szczęsna, A., Havel, L., Krzakowski, M., Hochmair, M.J., Huemer, F., Losonczy, G., Johnson, M.L., Nishio, M., et al. (2018). First-Line Atezolizumab plus Chemotherapy in Extensive-Stage Small-Cell Lung Cancer. N. Engl. J. Med. Overseas. Ed. *379*, 2220–2229. https://doi.org/10.1056/NEJMoa1809064.

56. Paz-Ares, L., Dvorkin, M., Chen, Y., Reinmuth, N., Hotta, K., Trukhin, D., Statsenko, G., Hochmair, M.J., Özgüroğlu, M., Ji, J.H., et al. (2019). Durvalumab plus platinum–etoposide versus platinum–etoposide in first-line treatment of extensive-stage small-cell lung cancer (CASPIAN): a randomised, controlled, open-label, phase 3 trial. Lancet *394*, 1929–1939. https://doi.org/10.1016/S0140-6736(19)32222-6.

57. Antonia, S.J., López-Martin, J.A., Bendell, J., Ott, P.A., Taylor, M., Eder, J.P., Jäger, D., Pietanza, M.C., Le, D.T., de Braud, F., et al. (2016). Nivolumab alone and nivolumab plus ipilimumab in recurrent small-cell lung cancer (CheckMate 032): a multicentre, open-label, phase 1/2 trial. Lancet Oncol. *17*, 883–895. https://doi.org/10.1016/S1470-2045(16)30098-5.

58. Rudin, C.M., Awad, M.M., Navarro, A., Gottfried, M., Peters, S., Csőszi, T., Cheema, P.K., Rodriguez-Abreu, D., Wollner, M., Yang, J.C.-H., et al. (2020). Pembrolizumab or Placebo Plus Etoposide and Platinum as First-Line Therapy for Extensive-Stage Small-Cell Lung Cancer: Randomized, Double-Blind, Phase III KEYNOTE-604 Study. J. Clin. Oncol. *38*, 2369–2379. https://doi.org/10.1200/JCO.20.00793.

59. Jarmoskaite, I., and Russell, R. (2011). DEAD-box proteins as RNA helicases and chaperones. WIREs RNA *2*, 135–152. https://doi.org/10.1002/wrna.50.

60. Mohibi, S., Chen, X., and Zhang, J. (2019). Cancer the'RBP'eutics–RNA-binding proteins as therapeutic targets for cancer. Pharmacol. Ther. *203*, 107390. https://doi.org/10.1016/j.pharmthera.2019.07.001.

61. Nyamao, R.M., Wu, J., Yu, L., Xiao, X., and Zhang, F.-M. (2019). Roles of DDX5 in the tumorigenesis, proliferation, differentiation, metastasis and pathway regulation of human malignancies. Biochim. Biophys. Acta Rev. Canc *1871*, 85–98. https://doi.org/10.1016/j.bbcan.2018.11.003.

62. Li, F., Fountzilas, C., Puzanov, I., Attwood, K.M., Morrison, C., and Ling, X. (2021). Multiple functions of the DEAD-box RNA helicase, DDX5 (p68), make DDX5 a superior oncogenic biomarker and target for targeted cancer therapy. Am. J. Cancer Res. *11*, 5190–5213.

63. Deng, X., Lin, N., Fu, J., Xu, L., Luo, H., Jin, Y., Liu, Y., Sun, L., and Su, J. (2020). The Nrf2/PGC1α Pathway Regulates Antioxidant and Proteasomal Activity to Alter Cisplatin Sensitivity in Ovarian. Cancer. Oxid. Med. Cell Longev. *2020*, 4830418. https://doi.org/10.1155/2020/4830418.

64. Lin, Y.-H., Lim, S.-N., Chen, C.-Y., Chi, H.-C., Yeh, C.-T., and Lin, W.-R. (2022). Functional Role of Mitochondrial DNA in Cancer Progression. Int. J. Mol. Sci. *23*, 1659. https://doi.org/10.3390/ijms23031659.

65. YUN, C.W., LEE, J.H., and LEE, S.H. (2019). Hypoxia-induced PGC-1α Regulates Mitochondrial Function and Tumorigenesis of Colorectal Cancer Cells. Anticancer Res. *39*, 4865–4876. https://doi.org/10.21873/anticanres.13672.

66. Boland, M.L., Chourasia, A.H., and Macleod, K.F. (2013). Mitochondrial Dysfunction in Cancer. Front. Oncol. *3*, 292. https://doi.org/10.3389/fonc.2013.00292.

67. Wu, N., Jiang, M., Han, Y., Liu, H., Chu, Y., Liu, H., Cao, J., Hou, Q., Zhao, Y., Xu, B., and Xie, X. (2019). O-GlcNAcylation promotes colorectal cancer progression by regulating protein stability and potential catcinogenic function of DDX5. J. Cell Mol. Med. *23*, 1354–1362. https://doi.org/10.1111/jcmm.14038.

68. Li, Y., Xing, Y., Wang, X., Hu, B., Zhao, X., Zhang, H., Han, F., Geng, N., Wang, F., Li, Y., et al. (2021). PAK5 promotes RNA helicase DDX5 sumoylation and miRNA-10b processing in a kinase-dependent manner in breast cancer. Cell Rep. *37*, 110127. https://doi.org/10.1016/j.celrep.2021.110127.

69. van Meerbeeck, J.P., and Ball, D. (2015). Small-cell lung cancer: local therapy for a systemic disease? Lancet *385*, 9–10. https://doi.org/10.1016/S0140-6736(14)61252-6.

70. Lu, Y., Li, H., Zhao, P., Tian, L., Liu, Y., Sun, X., and Cheng, Y. (2024). Dynamic phenotypic reprogramming and chemoresistance induced by lung fibroblasts in small cell lung cancer. Sci. Rep. *14*, 2884. https://doi.org/10.1038/s41598-024-52687-z.

71. Cheng, Y., Han, L., Wu, L., Chen, J., Sun, H., Wen, G., Ji, Y., Dvorkin, M., Shi, J., Pan, Z., et al. (2022). Effect of First-Line Serplulimab vs Placebo Added to Chemotherapy on Survival in Patients With Extensive-Stage Small Cell Lung Cancer. JAMA *328*, 1223–1232. https://doi.org/10.1001/jama.2022.16464.

72. Paz-Ares, L., Chen, Y., Reinmuth, N., Hotta, K., Trukhin, D., Statsenko, G., Hochmair, M.J., Özgüroğlu, M., Ji, J.H., Garassino, M.C., et al. (2022). Durvalumab, with or without tremelimumab, plus platinum-etoposide in first-line treatment of extensive-stage small-cell lung cancer: 3-year overall survival update from CASPIAN. ESMO Open *7*, 100408. https://doi.org/10.1016/j.esmoop.2022.100408.

73. Kalainayakan, S.P., FitzGerald, K.E., Konduri, P.C., Vidal, C., and Zhang, L. (2018). Essential roles of mitochondrial and heme function in lung cancer bioenergetics and tumorigenesis. Cell Biosci. *8*, 56. https://doi.org/10.1186/s13578-018-0257-8.

74. Courtnay, R., Ngo, D.C., Malik, N., Ververis, K., Tortorella, S.M., and Karagiannis, T.C. (2015). Cancer metabolism and the Warburg effect: the role of HIF-1 and PI3K. Mol. Biol. Rep. *42*, 841–851. https://doi.org/10.1007/s11033-015-3858-x.

75. Phan, L.M., Yeung, S.-C.J., and Lee, M.-H. (2014). Cancer metabolic reprogramming: importance, main features, and potentials for precise targeted anti-cancer therapies. Cancer Biol. Med. *11*, 1–19. https://doi.org/10.7497/j.issn.2095-3941.2014.01.001.

76. Cairns, R.A., Harris, I.S., and Mak, T.W. (2011). Regulation of cancer cell metabolism. Nat. Rev. Cancer *11*, 85–95. https://doi.org/10.1038/nrc2981.

77. Hensley, C.T., Faubert, B., Yuan, Q., Lev-Cohain, N., Jin, E., Kim, J., Jiang, L., Ko, B., Skelton, R., Loudat, L., et al. (2016). Metabolic Heterogeneity in Human Lung Tumors. Cell *164*, 681–694. https://doi.org/10.1016/j.cell.2015.12.034.

78. Davidson, S.M., Papagiannakopoulos, T., Olenchock, B.A., Heyman, J.E., Keibler, M.A., Luengo, A., Bauer, M.R., Jha, A.K., O'Brien, J.P., Pierce, K.A., et al. (2016). Environment Impacts the Metabolic Dependencies of Ras-Driven Non-Small Cell Lung Cancer. Cell Metab. *23*, 517–528. https://doi.org/10.1016/j.cmet.2016.01.007.

79. Rao, S., Mondragón, L., Pranjic, B., Hanada, T., Stoll, G., Köcher, T., Zhang, P., Jais, A., Lercher, A., Bergthaler, A., et al. (2019). AIF-regulated oxidative phosphorylation supports lung cancer development. Cell Res. *29*, 579–591. https://doi.org/10.1038/s41422-019-0181-4.

80. Faubert, B., Li, K.Y., Cai, L., Hensley, C.T., Kim, J., Zacharias, L.G., Yang, C., Do, Q.N., Doucette, S., Burguete, D., et al. (2017). Lactate Metabolism in Human Lung Tumors. Cell *171*, 358–371.e9. https://doi.org/10.1016/j.cell.2017.09.019.

81. Pastò, A., Bellio, C., Pilotto, G., Ciminale, V., Silic-Benussi, M., Guzzo, G., Rasola, A., Frasson, C., Nardo, G., Zulato, E., et al. (2014). Cancer stem cells from epithelial ovarian cancer patients privilege oxidative phosphorylation, and resist glucose deprivation. Oncotarget *5*, 4305–4319. https://doi.org/10.18632/oncotarget.2010.

82. Vlashi, E., Lagadec, C., Vergnes, L., Matsutani, T., Masui, K., Poulou, M., Popescu, R., Della Donna, L., Evers, P., Dekmezian, C., et al. (2011). Metabolic state of glioma stem cells and nontumorigenic cells. Proc. Natl. Acad. Sci. USA *108*, 16062–16067. https://doi.org/10.1073/pnas.1106704108.

83. Lagadinou, E.D., Sach, A., Callahan, K., Rossi, R.M., Neering, S.J., Minhajuddin, M., Ashton, J.M., Pei, S., Grose, V., O'Dwyer, K.M., et al. (2013). BCL-2 inhibition targets oxidative phosphorylation and selectively eradicates quiescent human leukemia stem cells. Cell Stem Cell *12*, 329–341. https://doi.org/10.1016/j.stem.2012.12.013.

84. Gao, C., Shen, Y., Jin, F., Miao, Y., and Qiu, X. (2016). Cancer Stem Cells in Small Cell Lung Cancer Cell Line H446: Higher Dependency on Oxidative Phosphorylation and Mitochondrial Substrate-Level Phosphorylation than Non-Stem Cancer Cells. PLoS One *11*, e0154576. https://doi.org/10.1371/journal.pone.0154576.

85. Gao, S.-P., Sun, H.-F., Fu, W.-Y., Li, L.-D., Zhao, Y., Chen, M.-T., and Jin, W. (2017). High expression of COX5B is associated with poor prognosis in breast cancer. Future Oncol. *13*, 1711–1719. https://doi.org/10.2217/fon-2017-0058.

86. Gao, S.-P., Sun, H.-F., Jiang, H.-L., Li, L.-D., Hu, X., Xu, X.-E., and Jin, W. (2015). Loss of COX5B inhibits proliferation and promotes senescence via mitochondrial dysfunction in breast cancer. Oncotarget *6*, 43363–43374. https://doi.org/10.18632/oncotarget.6222.

87. Lissa, D., Takahashi, N., Desai, P., Manukyan, I., Schultz, C.W., Rajapakse, V., Velez, M.J., Mulford, D., Roper, N., Nichols, S., et al. (2022). Heterogeneity of neuroendocrine transcriptional states in metastatic small cell lung cancers and patient-derived models. Nat. Commun. *13*, 2023. https://doi.org/10.1038/s41467-022-29517-9.

88. Drapkin, B.J., George, J., Christensen, C.L., Mino-Kenudson, M., Dries, R., Sundaresan, T., Phat, S., Myers, D.T., Zhong, J., Igo, P., et al. (2018). Genomic and Functional Fidelity of Small Cell Lung Cancer Patient-Derived Xenografts. Cancer Discov. *8*, 600–615. https://doi.org/10.1158/2159-8290.CD-17-0935.

89. Vidhyasagar, V., Haq, S.U., and Lok, B.H. (2020). Patient-derived Xenograft Models of Small Cell Lung Cancer for Therapeutic Development. Clin. Oncol. *32*, 619–625. https://doi.org/10.1016/j.clon.2020.05.017.

90. Borowicz, S., Van Scoyk, M., Avasarala, S., Karuppusamy Rathinam, M.K., Tauler, J., Bikkavilli, R.K., and Winn, R.A. (2014). The Soft Agar Colony Formation Assay. J. Vis. Exp. *92*, e51998. https://doi.org/10.3791/51998.

91. Bustin, S.A., Benes, V., Garson, J.A., Hellemans, J., Huggett, J., Kubista, M., Mueller, R., Nolan, T., Pfaffl, M.W., Shipley, G.L., et al. (2009). The MIQE Guidelines: Minimum Information for Publication of Quantitative Real-Time PCR Experiments. Clin. Chem. *55*, 611–622. https://doi.org/10.1373/clinchem.2008.112797.

92. Robinson, M.D., McCarthy, D.J., and Smyth, G.K. (2010). edgeR: a Bioconductor package for differential expression analysis of digital gene expression data. Bioinformatics *26*, 139–140. https://doi.org/10.1093/bioinformatics/btp616.

93. Love, M.I., Huber, W., and Anders, S. (2014). Moderated estimation of fold change and dispersion for RNA-seq data with DESeq2. Genome Biol. *15*, 550. https://doi.org/10.1186/s13059-014-0550-8.

STAR★METHODS

KEY RESOURCES TABLE

REAGENT or RESOURCE	SOURCE	IDENTIFIER
Antibodies		
Mouse anti-β-Catenin monoclonal antibody (CAT-5H10)	Invitrogen	Cat#13–8400; RRID: AB_2533039
Rabbit anti-DDX5 monoclonal antibody (EPR7239)	Abcam	Cat#ab126730; RRID: AB_11130291
Rabbit anti-RFC1 polyclonal antibody	Abcam	Cat#ab3853; RRID: AB_2238314
Rabbit anti-DDX5 polyclonal (phospho Y593) antibody	Abcam	Cat#ab62255; RRID: AB_942233
Rabbit anti-c-Myc (D84C12) monoclonal antibody	Cell Signaling Technology	Cat#5605; RRID: AB_1903938
Mouse anti-β-Actin monoclonal antibody	Sigma-Millipore	Cat#A5441; RRID: AB_476744
Goat anti-Rabbit IgG (H + L) Secondary Antibody, HRP	Invitrogen	Cat#31460; RRID: AB_228341
Peroxidase AffiniPure™ Goat Anti-Mouse IgG (H + L)	Jackson ImmunoResearch Laboratories Inc.	Cat#115-035-003; RRID: AB_10015289
Biological samples		
Patient-derived xenografts (PDX)	The Jackson laboratory	TM00194 (https://tumor.informatics.jax.org/mtbwi/pdxDetails.do?modelID=TM00194)
Chemicals, peptides, and recombinant proteins		
RPMI 1640 medium	ATCC	30–2001
DMEM medium	ATCC	30–2002
Keratinocyte-SFM medium	Gibco, Life Technologies	17005042
Penicillin-Streptomycin (10,000 U/mL)	Gibco, Life Technologies	15140122
Fetal Bovine Serum - Premium	Biotechne (R&D systems)	S11150
Supinoxin (RX-5902)	ChemieTek	CT-RX5902
TRIzol™ Reagent	Invitrogen	15596026
SYBR™ Green Universal Master Mix	Applied Biosystems	4309155
TrypLE™ Express Enzyme (1X), phenol red	Gibco, Life Technologies	12605010
Cell Lysis Buffer (10X)	Cell Signaling Technology	9803
cOmplete™, EDTA-free Protease Inhibitor Cocktail	Roche, Sigma Millipore	11873580001
Immobilon® Crescendo Western HRP substrate	Sigma-Millipore	WBLUR0500
VECTASTAIN® Elite® ABC-HRP Kit, Peroxidase (Standard)	Vector Laboratories	PK-6100
DAB Substrate Kit, Peroxidase (HRP), with Nickel, (3,3′-diaminobenzidine)	Vector Laboratories	SK-4100
Harris Hematoxylin Solution, Modified	Sigma-Millipore	HHS16
Fisher Chemical™ Permount™ Mounting Medium	Fisher Scientific	SP15-100
Seahorse XFp Media & Calibrant	Agilent	103681–100
Critical commercial assays		
CyQUANT™ Direct Cell Proliferation Assay	Invitrogen	C35011
QuantiTect Reverse Transcription Kit	Qiagen	205310
Seahorse XF Cell Mito Stress Test Kit	Agilent	103015–100
PCR Mycoplasma Detection Kit	Applied Biological Mat. Inc.	G238
Deposited data		
RNA Sequencing	NCBI Gene Expression Omnibus (*this study)	GSE255741
RNA Sequencing	NCBI Gene Expression Omnibus (Xing et al.[27])	GSE142024

(*Continued on next page*)

Continued

REAGENT or RESOURCE	SOURCE	IDENTIFIER
RNA Sequencing	NCBI Gene Expression Omnibus (Sato et al.[35])	GSE43346 (GDS4794/225886_at)
Original Western Blot Data	Mendeley Data (*this study)	https://doi.org/10.17632/r6ryb6ckps.1
Experimental models: Cell lines		
HBEC-3KT	Gift from Andrea Kasinski (Purdue University)	N/A
NCI-H69 (H69)	ATCC	HTB-119
NCI-H69AR (H69AR)	ATCC	CRL-11351
MDA-MB-231	Gift from Michael Wendt (Purdue University)	N/A
Oligonucleotides		
Primer for RT-qPCR	This paper	Table S1
Software and algorithms		
GraphPad Prism	GraphPad	version 9.3.0
Gene Expression Profiling Interactive Analysis (GEPIA)	http://gepia.cancer-pku.cn/	N/A
TrimGalore toolkit	https://www.bioinformatics.babraham.ac.uk/projects/trim_galore/	version 0.4.4
R-software	the R Core Team and the R Foundation for Statistical Computing	version 4.3.3
Tableau	Salesforce	version 2023.3.0

EXPERIMENTAL MODEL AND STUDY PARTICIPANT DETAILS

Cell lines

Human SCLC cell lines NCI-H69 (H69) and NCI-H69AR (H69AR) cells were purchased from American Type Culture Collection (ATCC). HBEC-3KT (HBEC) cell line was a gift from Dr. Andrea Kasinski (Purdue University). The triple negative breast cancer cell line, MDA-MB-231 cell line was a gift from Dr. Michael Wendt (Purdue University). H69 cells were grown in RPMI 1640 medium (ATCC, 30–2001) with 10% fetal bovine serum (FBS; Biotechne R&D systems, S11150) and 1% penicillin-streptomycin solution (Gibco, Life Technologies, 15140122). H69AR cells were grown in RPMI 1640 medium with 20% fetal bovine serum and 1% penicillin-streptomycin solution. MDA-MB-231 cells were cultivated in Dulbecco's Modified Eagle's Medium (DMEM; ATCC, 30–2002) with 10% fetal bovine serum and 1% penicillin-streptomycin solution. HBEC-3KT cells were grown in Keratinocyte-SFM medium (Gibco, Life Technologies 17005042) supplemented with bovine pituitary extract (BPE), human recombinant epidermal growth factor (rEGF) and 1% penicillin-streptomycin solution. All cell lines were cultured at 37°C in a humidified environment, supplemented with 5% CO_2. All cell lines were systematically and routinely tested for the absence of mycoplasma contamination using the PCR Mycoplasma Detection Kit (Applied Biological Mat. Inc., G238).

Animal experiments

Severely immunocompromised NRG mice (The Jackson Laboratory stock #007799) 10–16 weeks old (male or female) were used for all tumor implantations. Tumor volume was measured with digital calipers by taking 3 perpendicular measurements of LxWxH. Mice were monitored 2×/week for tumor growth and weight gain/loss and were euthanized when tumor volume reached 2000 mm^3 or if other humane criteria were met. H69AR cells still in log-phase growth were harvested from culture flasks and injected subcutaneously in the flank at 5 × 10^6 cells/mouse using a 25 ga needle. Cells were mixed 1:1 with Matrigel (50 μL:50 μL) for injection in mice. PDX tumors were implanted subcutaneously in the flank after harvesting tumors from donor mice. Donor tumors were minced into a paste with a razor blade, large fibrous chunks were removed, and the remaining paste was mixed 1:1 with Matrigel (50 μL:50 μL) for injection with 14 ga needles in mice. PDX tumors were purchased from the Jackson Laboratory (PDX# TM00194). It is a pleural effusion sample. The details can be found at https://tumor.informatics.jax.org/mtbwi/pdxDetails.do?modelID=TM00194.

Ethics committee approval

All animal experiments were approved by the Purdue Institutional Animal Care and Use Committee prior to initiating studies. The protocol #1112000342 was approved 1/16/2022. The studies were also approved by the Purdue University Institutional Biosafety

Committee protocol #12-007, approved 2/3/2019. All animal procedures and euthanasia were performed consistent with the recommendations of the panel of the American Veterinary Medical Association. All mice used in the studies were 10–16 weeks old, and both males and females were used (not all studies are shown).

METHOD DETAILS

Growth analysis

H9 and H69AR cells were seeded at a density of 10000 cells per well in 96-well plates (Corning, 3603). Supinoxin (ChemieTek, CT-RX5902) was dissolved in DMSO in order to prepare a stock solution of 5mM. Following a 24-h growth period, cells were treated with different concentrations of Supinoxin (0, 0.1, 1, 5, 10, 20, 40, 70, 100 and 1000 nM) diluted in appropriate growth media. The CyQUANT direct cell proliferation kit (Invitrogen, C35011) was then used to measure the number of live cells. Relative fluorescence was calculated after subtracting background fluorescence from unlabeled cells. Soft agar assays were carried out as described.[90] GraphPad Prism 9 was used to determine the IC_{50} (half maximal inhibitory concentration) of Supinoxin.

RT-qPCR

TRIzol Reagent (Invitrogen, 15596026) was used to extract total RNA from H69AR and MDA-MB-231 cells. cDNAs were then prepared from total RNA using the QuantiTect kit (Qiagen, 205310). To examine the expression levels of particular mRNAs, qPCR was carried out using SYBR green master mix (Applied Biosystems, 4309155) (Table S1 showing the list of primers used for the study). The relative expression level of specific RNAs was calculated using the Pfaffl method using the reference gene glyceraldehyde-3-phosphate dehydrogenase. RT-qPCRs were performed using MIQE guidelines.[91]

Western Blot

MDA-MB-231 and H69AR cells were seeded and allowed to adhere for 24 h in 6-well plates. Supinoxin was dissolved in DMSO in order to prepare a stock solution at 100μM. Cells were treated with different concentrations of Supinoxin (0, 20, 70, or 100 nM) diluted in appropriate growth media for 24 to 48 h. Cells were then trypsinized and collected using 1X TrypLE Express (Gibco, Life Technologies 12605010) followed by lysis in Cell Lysis Buffer (Cell Signaling Technology, 9803), with EDTA-free protease inhibitor cocktail (Roche, Sigma Millipore, 11873580001). 20–50 mg of total protein was loaded onto an 8% SDS-PAGE gel, which was then electrophoresed and transferred to nitrocellulose membrane using the Mini PROTEAN Tetra Cell device (Bio-Rad). After being blocked in 2% skimmed milk for 5 min, membranes were incubated at 4°C overnight with primary antibodies β-catenin (Invitrogen, 13–8400), DDX5 (Abcam, ab126730), RFC1 (Abcam, ab3853), phosphor-DDX5 (Y593) (Abcam, ab62255), c-Myc (Cell Signaling Technology, 5605), β-Actin (Sigma-Millipore, A5441). HRP-conjugated secondary antibodies were used to image western blots: anti-rabbit (Invitrogen, 31460) anti-mouse (Jackson ImmunoResearch, 115-035-003). The blots were detected using Milipore Immobilon Crescendo Western HRP Substrate reagent (Sigma-Millipore, WBLUR0500).

Microscopy

Cells were seeded onto glass coverslips coated with poly-L-lysine and given 24 h to adhere. Following a 24-h period (or as specified) of treatment with Supinoxin at increasing concentrations (0, 20, 70, or 100 nM), the cells were fixed with 1.6% formaldehyde in Phosphate Buffered Saline (PBS) (1:10 dilution of stock in PBS). Cells were then blocked with 2% BSA followed by incubation with primary antibodies for 2 h. Primary antibodies include phosphor-DDX5 Y593 (Abcam, ab62255) and β-catenin (Invitrogen, 13–8400). DNA was stained with 300 nM DAPI to serve as a nuclear marker. Cells were visualized using a Leica DM6 microscope with a 40× objective.

Histological staining

Histological staining was performed on paraffin-embedded samples of SCLC PDX and normal lung tissues. Tissue sections were taken at a thickness of 4 μm using a microtome (Thermo Scientific, HM355S). Sections were mounted on charged slides and dried on a 60°C oven. Slides were cleaned three times in xylene to deparaffinize the samples. Slides were then rehydrated by being submerged in decreasing concentrations of ethanol (100, 90, 70, 35%) followed by water Antigen unmasking was performed by pressure cooking slides for 20 min in a buffer made from Tris Base (1M), EDTA (100mM), and Tween 20 (5%), with a pH adjusted to 9.0. Slides were then cleaned with TBST three times before being incubated in 3% hydrogen peroxide for 5 min. After an additional wash in TBST, sections were blocked using 2.5% goat serum in 1X TBST for 20min in a humidified chamber. Primary antibody diluted in blocking solution was added to each section followed by incubation for 30 min at room temperature in a humidified box. Sections were washed once more in TBST and then incubated with secondary antibody in blocking solution for 30 min at room temperature in a humidified chamber. ABC Reagent (Vector Laboratories, PK-6100) and DAB Stock Solution (Vector Laboratories, SK-4100) kits were used in accordance with the manufacturer's instructions to stain the section. Hematoxylin (Sigma-Millipore, HHS16) was then used to counterstain the sections for 1 min. The sections were then dehydrated by washing in increasing concentrations of ethanol (95 and 100% ethanol), followed by a xylene wash. Coverslips were then mounted onto slides using Permount (Fischer Scientific, SP15-100). Images were taken using a Leica DM6 microscope with a 10× objective.

RNA-seq and data analysis

Three biological replicates of H69AR cells treated with or without 70nM of Supinoxin were used for RNA sequencing. Total RNA extraction was performed using TRIzol Reagent (Invitrogen, 15596026). Library construction and RNA sequencing were performed by Novogene Co., Ltd., Beijing, China. The libraries were sequenced using Illumina NovaSeq PE150 cassettes for paired-end sequencing with a 150-bp read length. Data quality control was conducted using the TrimGalore toolkit (version 0.4.4) (RRID:SCR_011847), with a minimum Phred score of 30 and a minimum read length of 50 bp. The quality trimmed reads were aligned to the human reference genome (GRCh38) obtained from the Ensembl database. The RNA-seq protocol included quality control (FastQC), trimming (Trimmomatic), alignment (HISAT2), and quantification (Feature Counts) in a bash (Linux) environment. Differential expression analysis was performed using both DESeq2 and edgeR methods.[92,93] The analysis identified genes that were significantly differentially expressed (DEGs) based on a false discovery rate (FDR) threshold of <0.05. The DESeq2 object included a pool of 3495 DEGs, which were used to investigate Gene Ontology (GO) and KEGG pathways. The oxidative phosphorylation pathway was visually represented using Pathview and the gage package, while GSEA conducted a comprehensive enrichment analysis of oxidative phosphorylation. The heatmap was created using heatmap and the Complex Heatmap package in R-Studio. The pathways' direction was determined by utilizing the assigned Z-scores. The volcano plot was prepared using the Enhanced Volcano package in RStudio. In addition, the comparison table for the enrichment pathway was created using Tableau Desktop Public Version 2023.3.0, incorporating KEGG data from Supinoxin treatment and DDX5 knockdown.[27]

Seahorse assay

H69AR cells were seeded in a 24-well microplate (Seahorse Bioscience) at a density of 20,000 cells per well and allowed to incubate in a standard 37°C CO_2 incubator overnight. Before the experiment, cells underwent two washes with Assay Media (Seahorse Bioscience) and were then incubated in a 37°C non-CO_2 incubator with 500 μL Assay Media per well for 1 h. The mitochondrial profile was assessed by measuring the oxygen consumption rates (OCR) using the Mito Stress Test Kit (Seahorse Bioscience). The OCR was calculated using the Seahorse XF Stress Test Report Generator (Seahorse Bioscience).

QUANTIFICATION AND STATISTICAL ANALYSIS

Figures were plotted using Prism 9.0 (version 9.3.0). The data from Figures 1, 2, 4A, 5A, and 9 were presented as mean ± standard SD. Student's T-test was utilized for comparisons between the two groups. The IC_{50} values presented in Figure 2 were determined using GraphPad Prism 9 software. The P- values are *<0.05, **<0.005, and ***<0.001; ns, not significant. The statistics for Figure 3A were calculated using Tukey's multiple comparisons test. The statistical evaluation for Figure 3C was performed using the log rank Mantel-Cox test. The statistical evaluation for Figure 3D was performed using the two-way ANOVA test. The data from Figures 4C–4E and 5C–5E were analyzed using one-way ANOVA for comparisons between two groups. Differences with P-values <0.05 were regarded as statistically significant.